

Development of NiCo₂O₄@SnS₂/CC nanostructures for high-performance supercapacitor



By

Maria Bibi

Registration No: 00000328686

Department of Materials Engineering

School of Chemical and Materials Engineering

National University of Sciences & Technology (NUST)

Islamabad, Pakistan

(2024)

Development of $\text{NiCo}_2\text{O}_4@ \text{SnS}_2/\text{CC}$ nanostructures for high-performance supercapacitor



By

Maria Bibi

Registration No: 00000328686

A thesis submitted to the National University of Sciences and Technology, Islamabad,

in partial fulfillment of the requirements for the degree of

Master of Science in
Nanoscience and Engineering

Supervisor: Dr. Amna Safdar

Co Supervisor (if any): Dr. Mashkoor Ahmad

School of Chemical and Materials Engineering

National University of Sciences & Technology (NUST)

Islamabad, Pakistan

(2024)



THESIS ACCEPTANCE CERTIFICATE

Certified that final copy of MS thesis written by Ms Maria Bibi (Registration No 00000328686), of School of Chemical & Materials Engineering (SCME) has been vetted by undersigned, found complete in all respects as per NUST Statues/Regulations, is free of plagiarism, errors, and mistakes and is accepted as partial fulfillment for award of MS degree. It is further certified that necessary amendments as pointed out by GEC members of the scholar have also been incorporated in the said thesis.

Signature: _____

Name of Supervisor: Dr Anna Safdar

Date: 04-07-2024

Signature (HOD): _____

Date: 04/07/24

Signature (Dean/Principal): _____

Date: 5/7/24



National University of Sciences & Technology (NUST)

FORM TH-4

MASTER'S THESIS WORK

We hereby recommend that the dissertation prepared under our supervision by

Regn No & Name: 00000328686 Maria Bibi

Title: Development of NiCo₂O₄@SnS₂/CC Nanostructures for High-performance Supercapacitor.

Presented on: 09 May 2024 at: 1430 hrs in SCME Seminar Hall

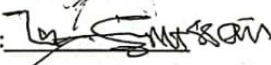
Be accepted in partial fulfillment of the requirements for the award of Masters of Science degree in Nanoscience & Engineering.

Guidance & Examination Committee Members

Name: Dr Muhammad Talha Masood

Signature: 

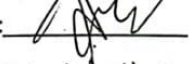
Name: Dr Zakir Hussain

Signature: 


Name: Dr Mashkoor Ahmad (Co-Supervisor)


Signature: 

Supervisor's Name: Dr Amna Safdar

Signature: 

Dated: 09 May 2024


Head of Department
Date 22/05/24


Dean/Principal
Date 22-5-2024

School of Chemical & Materials Engineering (SCME)



Form TH-1

(Must be type written)

National University of Sciences & Technology (NUST)
MASTER'S THESIS WORK

Formulation of Guidance and Examination Committee (GEC)

Name: Maria Bibi

NUST Regn No: 00000328686

Department: SCME

Specialization: MS In Nanoscience & Engineering

Credit Hour Completed: 18/24

CGPA: 3.58/3.50

Course Work Completed

S/No	Code	Title	Core/Elective	CH	Grade
1	MSE-856	Nanomaterials and Processing	Core	3	B+
2	MSE-854	Characterization of Materials	Core	3	B
3	NSE-813	Essentials of Nanoscience and Engineering	Core	3	B+
4	NSE-845	Nanolithography and Device Fabrication	Elective	3	A
5	MSE-872	Composite Materials	Elective	3	B+
6	NSE-812	Environmental Nanotechnology	Elective	3	A
7	RM-898	Research Methodology	Elective	3	Q
8	<u>NS2-842</u>	<u>Nano Materials for Energy Application</u>	<u>Elective</u>	<u>3</u>	<u>B+</u>
9	<u>NS2-843</u>	<u>Nano Technology & Photovoltaics</u>	<u>" "</u>	<u>3</u>	<u>B</u>

Date: 10th February, 2022

Student's Signature: Amna

Thesis Committee

- Name: Dr. Amna Safdar (Supervisor) Signature: [Signature]
Department: SCME
- Name: Dr. Mashkoor Ahmad (Co-Supervisor, if appointed) Signature: [Signature]
Department: PINSTECH
- Name: Dr. Zakir Hussain Signature: [Signature]
Department: SCME
- Name: Dr. Muhammad Talha Masood Signature: [Signature]
Department: SCME

Date: 18-4-22

Signature of Head of Department: [Signature]

APPROVAL

Date: 18-4-2022

Dean/Principal

Distribution

- 1x copy to Exam Branch, Main Office NUST
- 1x copy to PGP Dte, Main Office NUST
- 1x copy to Exam branch, respective institute

School of Chemical and Materials Engineering (SCME) Sector H-12, Islamabad

AUTHOR'S DECLARATION

I Maria Bibi hereby state that my MS thesis titled “Development of NiCo₂O₄@SnS₂/CC nanostructures for high-performance supercapacitor” is my own work and has not been submitted previously by me for taking any degree from National University of Sciences and Technology, Islamabad or anywhere else in the country/ world.

At any time if my statement is found to be incorrect even after I graduate, the university has the right to withdraw my MS degree.

Name of Student: Maria Bibi

Date: 04/07/2024

PLAGIARISM UNDERTAKING

I solemnly declare that research work presented in the thesis titled “Development of NiCo₂O₄@SnS₂/CC nanostructures for high-performance supercapacitor” is solely my research work with no significant contribution from any other person. Small contribution/help wherever taken has been duly acknowledged and that complete thesis has been written by me.

I understand the zero tolerance policy of the HEC and National University of Sciences and Technology (NUST), Islamabad towards plagiarism. Therefore, I as an author of the above titled thesis declare that no portion of my thesis has been plagiarized and any material used as reference is properly referred/cited.

I undertake that if I am found guilty of any formal plagiarism in the above titled thesis even after award of MS degree, the University reserves the rights to withdraw/revoke my MS degree and that HEC and NUST, Islamabad has the right to publish my name on the HEC/University website on which names of students are placed who submitted plagiarized thesis.

Student Signature: _____ 

Name: _____ Maria Bibi

DEDICATION

This research is genuinely dedicated to my dear family, who have been a source of inspiration and courage when I felt like giving up, and who continue to give moral, spiritual, emotional, and financial support.

ACKNOWLEDGEMENTS

Alhamdulillah, I thank Allah SWT for His magnificence and for giving me the strength, good health, and courage that He has bestowed upon me, and the ability to learn and understand to complete this research project and thesis successfully. First and foremost, I want to thank my supervisor, Dr. Amna Safdar, for her expertise and support during my studies while. My second deepest gratitude goes to my co-supervisor, Dr. Mashkoor Ahmad from PINSTECH, provided me a chance to work in the prestigious national research institute and availed the facilities. He helped me solve every complicated problem I faced during my research period. He shared his ideas with me from time to time. He also motivated, guided me, and gave me full access to the lab facilities. Besides my co-supervisor, I'm also very grateful to other Scientists including Dr. Shafqat Karim, Dr. Amjad Nisar, Dr. Amina Zafar, and Dr. Shafqat Hussain, and who assisted me in completing this project. I would also like to thank my GEC committee members, Prof. Dr. Zakir Hussain and Assistant Prof. Dr. Muhammad Talha Masood. I feel honored that you have accepted to be on my committee. I want to convey my wholehearted gratitude to all the teachers I have learned from since childhood and everyone who has directly or indirectly helped me throughout my academic journey. Finally, and most importantly, I express my profound gratitude to my parents for their unconditional love, care, sacrifices, encouragement, emotional and financial support, and many prayers. This institute has provided me with an amazingly extraordinary experience with so many things to cherish within a very short span. Thank you for giving me so much in that period.

- Maria Bibi

TABLE OF CONTENTS

ACKNOWLEDGEMENTS	VIII
TABLE OF CONTENTS	IX
LIST OF TABLES	XII
LIST OF FIGURES	XIII
LIST OF SYMBOLS, ABBREVIATIONS AND ACRONYMS	XV
ABSTRACT	XVI
CHAPTER 1: INTRODUCTION	1
1.1 Background	1
1.1.1 Energy storage Systems	1
1.1.2 Batteries vs Supercapacitors	2
1.2 Supercapacitors	4
1.3 Classification of Supercapacitors	5
1.4 Why use a supercapacitor?	6
1.5 History of Supercapacitors	7
1.6 Applications of Supercapacitors	8
1.7 Working Principle of Supercapacitors	9
1.8 Material Attributes	12
1.8.1 Electrode Materials	12
1.8.2 Electrolyte	13
1.8.3 Separator	14
1.9 Limitations for Supercapacitors	14
1.10 What is NiCo₂O₄	15
1.10.1 Structure of NiCo ₂ O ₄	16
1.10.2 Advantages and Disadvantages of NiCo ₂ O ₄	18
1.11 What is SnS₂	18
1.11.1 Structure of SnS ₂	19
1.11.2 Advantages and Disadvantages of SnS ₂	20
1.12 Significance and Research Objectives Major Revision	21
1.12.1 Research Objectives	21
CHAPTER 2: LITERATURE REVIEW	22
2.1 Historical Background	22
2.2 Supercapacitors	23
2.2.1 Types of Supercapacitors	23
2.2.2 Electrical Double Layer Capacitor	23

2.2.3 Pseudo capacitors	23
2.2.4 Hybrid Capacitors	24
2.2.5 Composite Hybrid	25
2.2.6 Asymmetric Hybrid	25
2.2.7 Battery Type Hybrid	25
2.3 Common Electrode Materials used in supercapacitor	26
2.3.1 Carbon Materials used in supercapacitor	26
2.3.2 Metal Oxide	28
2.3.3 Conducting Polymers	28
2.3.4 Composites	29
2.4 Why Oxides and Sulphides as an Electrode Material	29
2.5 Binary Metal Oxides	31
CHAPTER 3: EXPERIMENTAL WORK	36
3.1 Reagents and materials	36
3.2 Synthesis of Materials	36
3.2.1 Treatment on Carbon-Cloth	36
3.2.2 Preparation of NiCo ₂ O ₄ nanostructures	37
3.2.3 Preparation of NiCo₂O₄@SnS₂ nanostructures	37
3.2.4 Fabrication of Working Electrode	38
CHAPTER 4: CHARACTERIZATION TECHNIQUES	39
4.1 Instrumentation and Measurements	39
4.2 Raman Spectroscopy	39
4.2.1 Working Principle	40
4.3 XRD (X-ray diffraction)	42
4.3.1 Working Principle	42
4.4 SEM (Scanning Electron Microscopy)	45
4.4.1 Working Principle	46
4.5 TEM (Transmission Electron Microscopy)	48
4.5.1 Applications of TEM	49
4.6 XPS (X-Ray Photoelectron Spectroscopy)	50
4.6.1 Basic Principle and Mechanism	50
4.7 Fourier Transform Infra-Red (FT-IR) Spectroscopy	52
4.7.1 Working Principle	53
4.8 Brunauer, Emmett and Teller Analysis (BET)	54
4.8.1 Working Principle	55
4.9 Electrochemical Characterization	57
4.9.1 Cyclic voltammetry (CV)	57
4.9.2. Working Principle	58
4.9.3 Interpretation	59
4.10 Galvanostatic Charge/Discharge Analysis (GCD)	60
4.10.1 Working Principle	60
4.10.2 Interpretation	61
4.11 Electrochemical Impedance Spectroscopy (EIS)	62
4.11.1 Working Principle	62

CHAPTER 5: RESULTS AND DISCUSSION	65
5.1 Morphological, Structural and Compositional analysis	65
5.1.1 X-Ray Diffraction Analysis (XRD)	65
5.1.2 Morphological Analysis	66
5.1.3 Fourier Transform Infra-Red Spectroscopy (FTIR)	69
5.1.4 RAMAN Analysis	70
5.1.5 X-ray Photoelectron Spectroscopy (XPS)	71
5.1.6 Brunauer, Emmett and Teller Analysis (BET)	73
5.2 Electrochemical Characterization Techniques	74
5.2.1 Cyclic Voltammetry (CV)	74
5.2.2 Galvanostatic Charge and Discharge (GCD)	76
5.2.3 Rate Performance	78
5.2.4 Cyclic Performance	79
5.2.5 Electrochemical Impedance Spectroscopy	84
CHAPTER 6: CONCLUSION AND FUTURE RECOMMENDATIONS	86
REFERENCES	87

LIST OF TABLES

Table 1: Some of the major properties of NiCo ₂ O ₄	16
Table 2: Some of the major properties of SnS ₂	19
Table 3: NiCo ₂ O ₄ and SnS ₂ based nanostructures.....	32
Table 4: Comparative analysis of various electrochemical materials used as an electrode for high performance supercapacitors.....	81

LIST OF FIGURES

Figure 1: The comparison of energy density and power density for different energy storage devices.....	3
Figure 2: The Architecture of a mechanism of Supercapacitor.....	5
Figure 3: The types of a supercapacitor.....	6
Figure 4: Schematic of conventional capacitor.....	10
Figure 5: The typical electrical double-layer capacitor.....	11
Figure 6: The Crystal structures of NiCo ₂ O ₄ unit cell.....	17
Figure 7: The Crystal structures of SnS ₂	20
Figure 8: The numbers of reported literature related to supercapacitors from 2005 to 2015.....	22
Figure 9: Schematic representation of three types of Supercapacitor (a) EDLCs (b) Pseudo capacitor (c) Hybrid Capacitor. Copyright 2018 by American Society of Civil Engineers.....	24
Figure 10: Preparation of NiCo ₂ O ₄ nanostructures.....	37
Figure 11: Preparation of NiCo ₂ O ₄ @SnS ₂ /CC nanostructures.....	38
Figure 12: Three types of scattering processes.....	41
Figure 13: X-ray diffraction by planes of crystal.....	43
Figure 14: X-ray diffraction Schematic.....	44
Figure 15: Illustration of SEM.....	45
Figure 16: Illustration of TEM.....	49
Figure 17: Illustration of XPS.....	52
Figure 18: Illustration of instrumentation of FTIR.....	54
Figure 19: Illustration of working of BET analysis.....	56
Figure 20: Illustration of three electrode system for various electrochemical characterization.....	57
Figure 21: Cyclic voltammogram for an electrochemically reversible redox process.....	60
Figure 22: Nyquist plot with key regions labelled.....	64
Figure 23: XRD Spectra of CC/NiCo ₂ O ₄ and CC/NiCo ₂ O ₄ @SnS ₂	65
Figure 24: (a,b) Low and high magnification SEM image of carbon fibres (c,d) SEM image of NiCo ₂ O ₄ nanostructures supported carbon fibres.....	66
Figure 25: (a, b) low and high SEM images of CC/NiCo ₂ O ₄ @SnS ₂ structures (c) corresponding EDX spectrum of CC/NiCo ₂ O ₄ @SnS ₂ structure (d, e) Low and high magnification TEM images (f, g) High resolution TEM images of CC/NiCo ₂ O ₄ @SnS ₂ structures.....	68
Figure 26: (a). STEM image of CC/NiCo ₂ O ₄ @SnS ₂ nanostructures (b-h)EDS elemental mapping analysis for Ni, Co, O, C, Sn and S in CC/NiCo ₂ O ₄ @SnS ₂ nanosheets.....	69
Figure 27: FTIR spectra of CC/NiCo ₂ O ₄ and CC/NiCo ₂ O ₄ @SnS ₂ structures.....	70
Figure 28: Raman spectra of CC/NiCo ₂ O ₄ and CC/NiCo ₂ O ₄ @SnS ₂ structures.....	71

Figure 29: The high-resolution XPS spectra of CC/NiCo ₂ O ₄ and CC/NiCo ₂ O ₄ @SnS ₂ nanostructures (a) C 1s (b) Ni 2p (c) Co 2p (d) O 1s (e) Sn 3d and (f) S 2p	73
Figure 30: BET specific surface area of CC/NiCo ₂ O ₄ and CC/NiCo ₂ O ₄ @SnS ₂ structures	74
Figure 31: (a) Comparison of CV curves of CC/NiCo ₂ O ₄ and CC/NiCo ₂ O ₄ @SnS ₂ electrodes (b-c) CV curves of CC/NiCo ₂ O ₄ and CC/NiCo ₂ O ₄ @SnS ₂ structures at different scan rates	76
Figure 32: (a) Comparison of GCD curves of CC/NiCo ₂ O ₄ and CC/NiCo ₂ O ₄ @SnS ₂ electrodes (b-c) GCD curves of CC/NiCo ₂ O ₄ and CC/NiCo ₂ O ₄ @SnS ₂ structures at different current densities	77
Figure 33: (a) Comparison of specific capacitance of CC/NiCo ₂ O ₄ and CC/NiCo ₂ O ₄ @SnS ₂ at different current densities of 2 to 10 Ag ⁻¹ (b) Comparison of the Ragone plots of CC/NiCo ₂ O ₄ and CC/NiCo ₂ O ₄ @SnS ₂ electrodes	79
Figure 34: Cyclic performance of CC/NiCo ₂ O ₄ and CC/NiCo ₂ O ₄ @SnS ₂ at 2 Ag ⁻¹	80
Figure 35: Comparison of the EIS curves of CC/NiCo ₂ O ₄ and CC/NiCo ₂ O ₄ @SnS ₂ electrodes; inset is the kinetic parameters of both electrodes.	85

LIST OF SYMBOLS, ABBREVIATIONS AND ACRONYMS

NiCo_2O_4	Nickel Cobal Oxide
SnS_2	Tin di-sulfide
CC	Carbon Cloth
XRD	X-ray Diffraction
FTIR	Fourier Transform Infrared Spectroscopy
EDS	Elemental Dispersive Spectroscopy
SEM	Scanning Electron Microscopy
TEM	Transmission Electron Microscopy
XPS	X-ray Photoelectron Spectroscopy
BET	Brunauer–Emmett–Teller
CV	Cyclic Voltammetry
GCD	Galvanic Charge Discharge
EIS	Electrochemical Impedance Spectroscopy

ABSTRACT

Renewable energy storage systems are gaining interest due to the depletion of non-renewable energy sources and environmental concerns, while wearable devices and hybrid electric cars demand innovative storage solutions. However, supercapacitors are now thought to be the most promising power source for a range of electronic devices. In this work, NiCo₂O₄@SnS₂ nanosheets were synthesized on carbon cloth by utilizing a simple hydrothermal technique. The developed electrode material (NiCo₂O₄@SnS₂ /CC) was investigated for the supercapacitor applications. The high specific surface area, enhanced kinetics, good synergy, and distinct architecture of NiCo₂O₄@SnS₂ nanosheets produce a large number of active sites with substantial energy storage potential. As a supercapacitor, the electrode exhibits improved capacitance of 655.7 F/g at a current density of 2 A/g as compared to NiCo₂O₄/CC (560 F/g). Moreover, the electrode achieves 95.3 % of its preliminary capacitance after 10,000 cycles at 2A/g. Our results show that NiCo₂O₄@SnS₂ /CC nanosheets could be attractive electrode material for the development of supercapacitors.

CHAPTER 1: INTRODUCTION

1.1 Background

Due to the continued depletion of non-renewable energy sources and significant concern over the global environmental impact of conventional energy technologies, renewable and sustainable energy storage systems have garnered much interest. Moreover, the high demand for creating wearable devices, and hybrid electric cars encourages scientists to create innovative energy storage technologies [1]. The primary electrochemical energy storage technologies are lithium-ion batteries (LIBs), sodium-ion batteries (SIBs), and supercapacitors (SCs). These technologies are notable due to their critical roles in a variety of industries [2]. The use of renewable energy sources successfully addressed environmental issues. However, the intermittent nature of renewable energy sources and the variable power demands of different economies prompted the establishment of energy storage systems (ESS) that might help balance supply and demand. Supercapacitors are now seen as the most promising power source for a variety of electronic gadgets. Therefore, the growing demand for high-performance supercapacitors is primarily driven by their potential applications in various fields. Supercapacitors offer unique advantages over traditional energy storage devices like batteries and capacitors, making them increasingly desirable for a range of applications.

1.1.1 Energy storage Systems

Supercapacitors are gaining attention as energy storage systems due to their ability to store and deliver energy quickly. They offer high power density, enabling rapid charging and discharging cycles, making them ideal for applications that require quick bursts of power. This includes regenerative braking systems in electric vehicles, grid stabilization, and backup power supplies. Moreover, boosting a vehicle's efficiency requires storing kinetic energy whenever it slows or stops. Although these tasks have been successfully carried out on a low-power scale using batteries, new techniques to boost efficiency will need large

amounts of power, which can only be provided by other energy storage technologies such as supercapacitors.

These have sparked substantial interest because of their high power, energy density, and extended cycle life, providing an excellent opportunity to develop more sophisticated hybrid ESS for both on-board and stationary applications.

1.1.2 Batteries vs Supercapacitors

Supercapacitors and batteries are both energy storage devices but differ in their working principles, energy storage mechanisms, and performance characteristics. Figure 1 shows that capacitors have maximum power densities up to 106 W/kg and the lowest energy densities over 10-2 Wh/kg [3]. In contrast to capacitors, batteries, and fuel cells have the highest energy density among the energy storage devices reviewed. Supercapacitors, on the other hand, have power density and energy density numbers that fall in between batteries and capacitors. As a result, higher power density allows them to charge and discharge quickly, frequently within seconds or minutes, while lower energy density permits them to retain less energy than batteries.

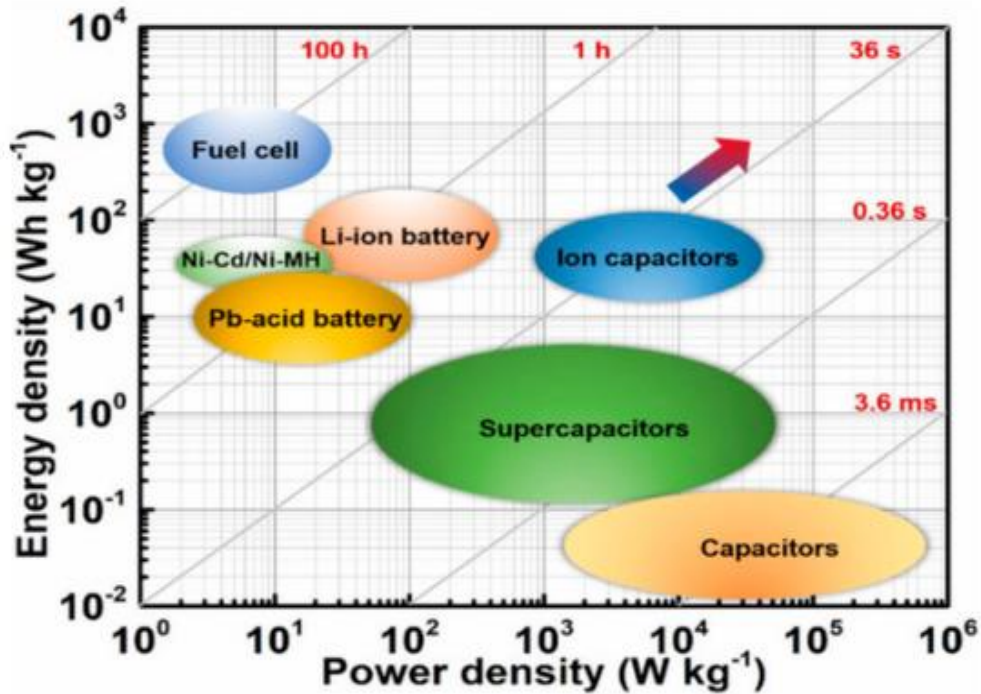


Figure 1: The comparison of energy density and power density for different energy storage devices.

- Working Principle:** Supercapacitors (also known as ultracapacitors or electrochemical capacitors) store energy electrostatically by separating positive and negative charges on the surface of electrodes. This process is known as the double-layer capacitance or electrochemical double-layer mechanism. Batteries, on the other hand, store energy chemically through a redox reaction. They involve the transfer of electrons between two electrodes through an electrolyte, which allows for the reversible conversion of chemical energy into electrical energy.
- Energy and Power Density:** Supercapacitors have high power density, enabling them to charge and discharge rapidly, often within seconds or minutes. However, they have lower energy density compared to batteries, meaning they can store a lower amount of energy per unit mass or volume. Batteries have relatively lower power density, leading to slower charging and discharging rates. However, they offer higher energy density, allowing them to store significantly more energy compared to supercapacitors.

- **Cycle Life and Lifespan:** Supercapacitors typically have a higher cycle life, meaning they can endure a large number of charge and discharge cycles without significant performance degradation. They can often sustain hundreds of thousands to millions of cycles. Batteries generally have a limited cycle life. The number of charge and discharge cycles they can withstand before experiencing a noticeable decline in performance depends on the battery chemistry and its specific design. The cycle life of batteries is usually in the range of hundreds to thousands of cycles.
- **Voltage Range:** Supercapacitors operate at low voltages, typically in the range of a few volts. They are often connected in series or parallel to achieve higher voltage or capacitance. Batteries, depending on their chemistry, can operate at higher voltages. The voltage output of batteries varies depending on the specific chemistry and configuration, ranging from a few volts to several hundred volts.
- **Application Scenarios:** Supercapacitors are suitable for applications requiring high power delivery and rapid energy transfer, such as regenerative braking systems in hybrid vehicles, peak power shaving in industrial applications, and short-term energy storage for renewable energy sources. Batteries are commonly used in applications that require higher energy storage capacity over longer durations, such as electric vehicles, portable electronic devices, grid energy storage, and off-grid renewable energy systems.

It is worth noting that recent advances in energy storage technologies have resulted in the creation of hybrid systems that combine the advantages of supercapacitors and batteries, intending to strike a balance between power density and energy density for specific applications.

1.2 Supercapacitors

A supercapacitor is composed of two electrodes, a separator, an electrolyte, and current collectors. These electrodes are mostly made of graphene and materials that resemble graphene, which have shown promise in terms of high power, density, and prolonged cycle life. This device has a significant energy storage capacity. It can store energy, has a high power density, and has a long cycle life [4]. Consumer electronics, electrical power grids,

transportation, and military applications, as well as different kinds of electrical instruments for commercial and industrial usage, are all anticipated to be influenced by supercapacitors.

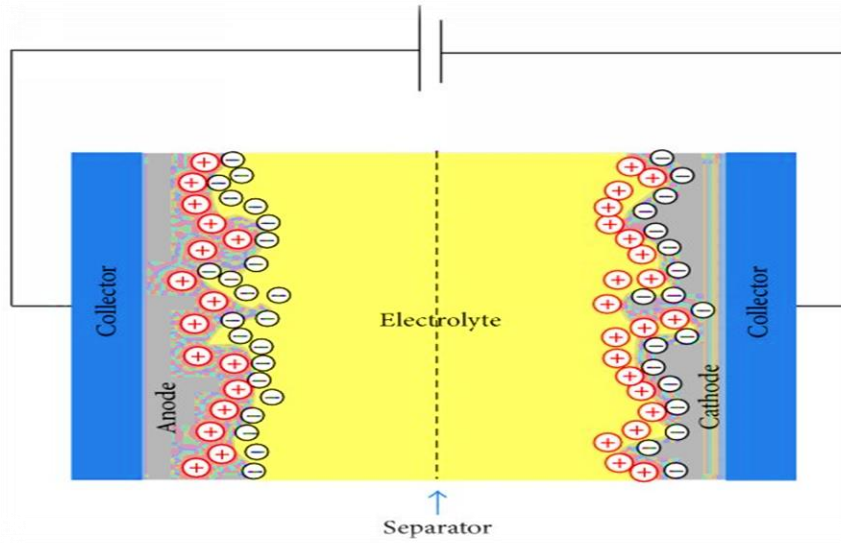


Figure 2: The Architecture of a mechanism of Supercapacitor.

1.3 Classification of Supercapacitors

Supercapacitors have distinct benefits over typical energy storage devices such as batteries and capacitors, making them more appealing for a variety of applications. They are categorized into the following various types based on the particular kind of electrode material used and their working principle:

- **EDLCs** (Electrical double-layer capacitors are based on carbon structures that employ non-faradic electrostatic charging of the electrical double-layer generated at the electrode-electrolyte interface [5].
- **Pseudo capacitors** (Pseudo capacitors are those which undergo fast and reversible faradic processes on the electrode materials when a potential is supplied, including the passage of charge across the double layer. Conducting polymers and several metal oxides, notably RuO_2 , MnO_2 , and Co_3O_4 , are among the materials undertaking such redox reactions.)

- **Hybrid capacitors** (Supercapacitors with high capacitance for long-term energy storage and pulse power can be created by combining faradaic and non-faradaic methods [6].

an asymmetric electrode arrangement in which one electrode is constructed of electrostatic carbon while the other is built of a faradaic capacitive substance. These supercapacitors are classified as hybrid/asymmetric supercapacitors.)

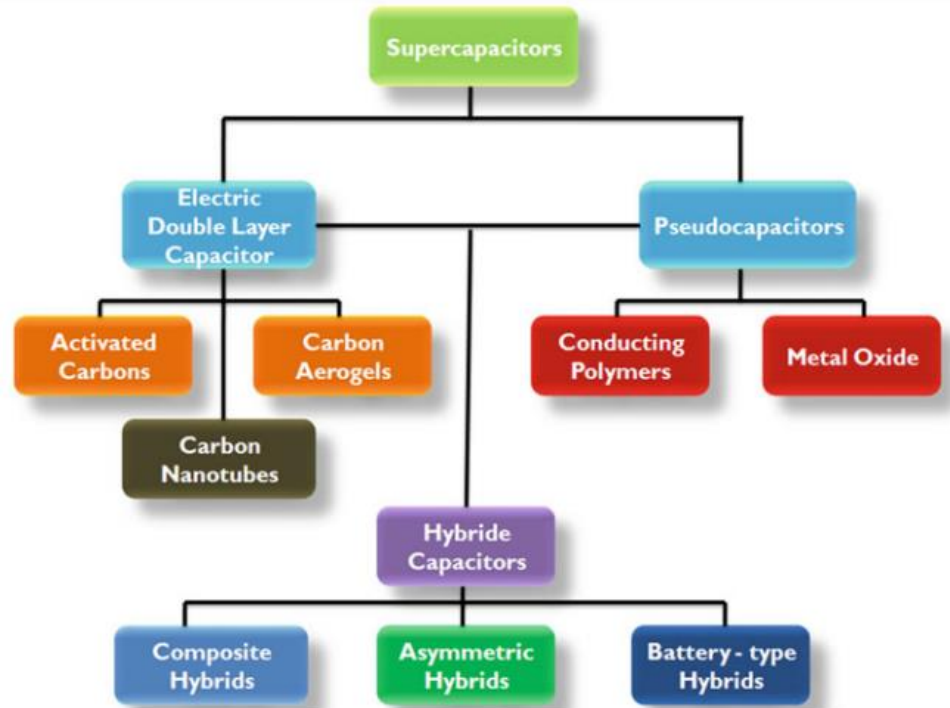


Figure 3: The types of a supercapacitor

1.4 Why use a supercapacitor?

The supercapacitor is currently the most promising energy storage device. The supercapacitor's long-term durability, high power density, and high energy properties make it suitable for auxiliary power units, backup power units, and power compensation [7]. A supercapacitor charges in 1-10 seconds. A supercapacitor's charge characteristics are similar, but the charge current is limited by the charger's current holding capacity. The potential energy deposits in the electric field in supercapacitors also, supercapacitors have a quicker charging and discharging capability making them more appealing than batteries.

Because the electrodes are highly absorbable materials, supercapacitors are designed to deliver (a) high power, (b) extended stability, and (c) efficient storage [8]. Heating hydrogen is used in the usage of a scalable nano-porous graphene manufacturing technique; graphene supercapacitors have a higher energy density than lithium batteries [9]. The supercapacitor is constructed of a spongy, porous substance with a very high specific area. The smaller the pores of the plates, the greater the ESR, and hence the lower the specific power.

A supercapacitor's reliability is defined as its ability to execute its function under specified operating circumstances and environments for a certain time. Supercapacitors have better reliability than batteries; batteries have 500-1000 charge/discharge cycles, but supercapacitors can endure for 5 to 10 years [10].

1.5 History of Supercapacitors

The perception of electrochemical supercapacitors (ESs) was caused by the electric double layer (EDL) that exists at the interface between a conductor and the electrolyte solution with which it interacts. In 1853, Hermann von Helmholtz first proposed the electric double-layer idea, which was later developed by Gouy, Chapman, Grahame, and Stern [11]. The term 'supercapacitor' is widely used, having originated as the trade name of the first commercial devices made by Nippon Electric Company (NEC) in 1971, and the term 'ultracapacitor' has also originated from devices made by Pinnacle Research Institute (PRI) with low internal resistance invented in 1982 for military applications.[12]R. A. Rightmire of Standard Oil of Ohio invented a device in 1966 that stored energy in a double-layer interface. In 1971, Nippon Electronic Company (NEC) of Japan manufactured aqueous-electrolyte capacitors for power-saving units in electronics under the license of the energy firm Standard Oil of Ohio, and this application was designated the commencement point for commercially based electrochemical capacitors (ECs) [13]. The growing proliferation of mobile phones, electronic devices, and electric vehicles has generated a need for innovative electrochemical energy storage systems with large power capacities. In the early 1990s, the US Department of Energy (DOE) expanded international awareness of the potential of supercapacitor and battery research, and it strongly promoted financing for

both. Tesla paid \$218 million for Maxwell Technologies, a well-known maker of ultracapacitors and storage materials. TESLA, Maxwell Technologies, Panasonic, Nesscap, EPCOS, NEC, ELNA, and TOKIN are among the companies making significant investments Reference? in electrochemical capacitor development today.

1.6 Applications of Supercapacitors

The globalized world faces increasing energy demand, power shortages, and high prices, driving research on advanced energy storage and management devices. Supercapacitors, known for their high power density, fast charging rate, and extended cycle life, are particularly attractive for high-pulse power and short-term power storage applications [14]. They have unique properties that make them suitable for a wide range of applications. Here are several key applications of supercapacitors:

- **Portable Power Supplies** (Electrochemical capacitors offer an effective alternative for standalone power sources, reducing charging time and improving efficiency.)
- **Consumer Electronics** (Supercapacitors find applications in consumer electronics for their ability to deliver high power bursts and long cycle life. They are used in devices such as digital cameras, laptops, smartphones, and wearables to provide quick energy boosts during peak demand, reducing strain on batteries and extending overall device life.)
- **Industrial Applications** (Supercapacitors are used in various industrial applications where high power density, rapid charge/discharge, and long cycle life are critical. They are employed in uninterruptible power supplies (UPS) to provide instantaneous power backup during power outages. Supercapacitors also find applications in robotics, automation, and manufacturing equipment where they can deliver high power bursts for motor startups, buffering intermittent loads, and managing energy fluctuations.)
- **Military and Aerospace Applications** (The military market segment is increasingly requiring ES devices to address power challenges due to their unique characteristics. These devices provide quick power delivery, a wide temperature range, and can handle up to a million cycles [15]. They are commonly used in backup power for electronics in vehicles, fire control systems, airbag deployments, helicopter black boxes, and

handheld radios. ES-based modules are also suitable for peak power applications, facilitating reliable communication transmission, active suspension, cold engine starts, and bus voltage hold-up during peak currents.)

- **Medical Devices** (Supercapacitors are used in various medical devices, such as pacemakers and implantable defibrillators, where reliability and long service life are crucial. They provide backup power during critical situations and can be rapidly charged, ensuring the devices remain functional in emergency scenarios.)

1.7 Working Principle of Supercapacitors

The general chemistry of conventional capacitors uses insulating dielectric material to separate conducting electrodes, allowing opposite charges to accumulate on each electrode. This creates an electric field, enabling energy storage [16]. When an electric potential is supplied across a conductor, electrons start to move and charge builds up on each conductor. When the potential is removed, the conducting plates stay charged until they come back into contact, at which point energy is released. The capacity of a capacitor to store energy is determined by its capacitance, which is the maximum amount of charge that can be held concerning the strength of the applied potential. The two equations below are applied to an electrostatic capacitor.

$$E = \frac{1}{2} CV^2 \quad (1.2)$$

$$C = \frac{Q}{V} = \epsilon AD \quad (1.1)$$

The formula for capacitance is $C=Q/V$ where Q represents charge, V represents electric potential, ϵ represents dielectric constant, A represents conductor surface area, d represents dielectric thickness, and E represents potential energy.

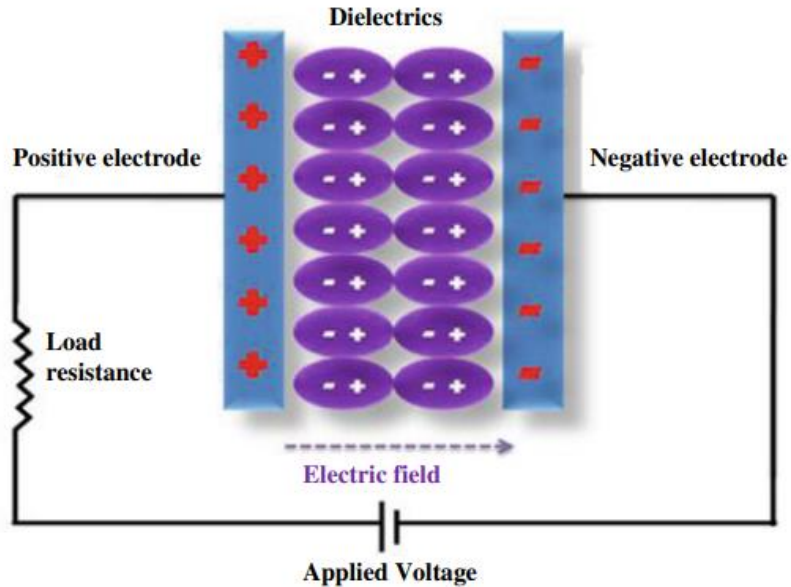


Figure 4: Schematic of conventional capacitor

The working principle of supercapacitors, also known as electrochemical capacitors, is based on the principles of double-layer capacitance and pseudocapacitance [17]. These two mechanisms contribute to the high energy storage capacity and rapid charge/discharge capabilities of supercapacitors.

- Double-Layer Capacitance:** The double-layer capacitance occurs at the interface between the electrode material and the electrolyte. When a voltage is applied across the supercapacitor electrodes, ions from the electrolyte are attracted to the oppositely charged electrode surfaces. This forms a double layer of separated charges: positive ions (cations) are adsorbed on the negatively charged electrode, while negative ions (anions) are adsorbed on the positively charged electrode. The separation of charges at the electrode-electrolyte interface creates an electric double layer, which acts as a dielectric material. This electric double-layer capacitance contributes to the overall capacitance of the supercapacitor. The electrode materials used in supercapacitors, such as activated carbon, have a high surface area and porosity, allowing for a larger interface area and greater charge separation.

- Pseudocapacitance:** Pseudocapacitance arises from fast and reversible faradaic reactions occurring at the electrode-electrolyte interface. Unlike double-layer capacitance, pseudocapacitance involves reversible redox reactions between the electrode material and the electrolyte. The electrode material undergoes surface-bound Faradaic reactions, where ions from the electrolyte are adsorbed or desorbed on the electrode surface. Pseudocapacitance can be achieved by using electrode materials that exhibit redox reactions, such as transition metal oxides (e.g. ruthenium oxide, manganese oxide) or conducting polymers (e.g. polyaniline, polypyrrole)[18]. These materials can store and release charge by the reversible transfer of electrons between the electrode and the electrolyte, contributing to the overall capacitance of the supercapacitor.
- Working Process:** When a supercapacitor is charged, electrons are forced onto one electrode, creating a negative charge, while the other electrode becomes positively charged. The charge separation occurs through the double-layer capacitance and, in the case of pseudocapacitive materials, through faradaic reactions. The energy is stored in the form of separated charges at the electrode-electrolyte interface.

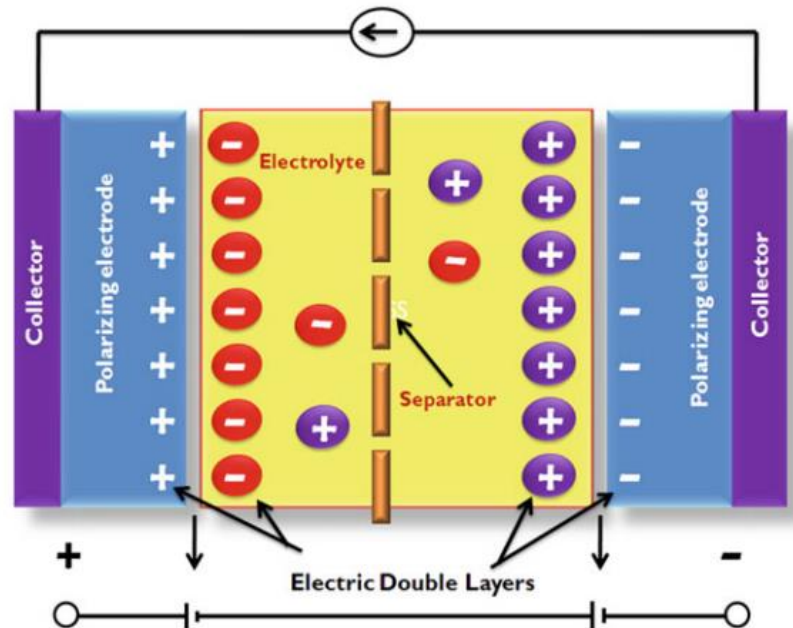


Figure 5: The typical electrical double-layer capacitor

During discharge, the stored energy is released as the separated charges neutralize each other. The electrons flow from the negatively charged electrode to the positively charged electrode through an external circuit, allowing the supercapacitor to deliver a high amount of power quickly [19]. The discharge process is rapid due to the ease with which the charges can move within the supercapacitor structure, providing high power density [20]. It's important to note that supercapacitors have higher power density but lower energy density compared to batteries. This means they can deliver high-power bursts rapidly but store less total energy. The working principle of supercapacitors enables them to have fast charge/discharge cycles, long cycle life, and high efficiency, making them suitable for applications requiring frequent power delivery and energy storage.

1.8 Material Attributes

The properties of a supercapacitor's material are essential to its performance. A supercapacitor's anode, cathode, and electrolyte materials must be chosen following the supercapacitor's functional requirements.

1.8.1 Electrode Materials

The electrode of a supercapacitor stores charge depending on its electrode-active materials, which require strong electrical conductivity, surface area, porous structure, and redox activity [21]. Selecting electrode-active materials is crucial for optimal performance; nanoscience advances enable the development of novel nanomaterials for supercapacitor applications. Nanostructured materials are preferred due to their distinct properties compared to macro- or microelectrode materials. These materials have good electrical conductivity, large surface area, thermal stability, and chemical resistance. The porous structure of electrode-active materials can be easily modified, and their large surface area allows for easy diffusion of electrolytes, enhancing performance [22]. Supercapacitor devices use electrode materials like carbon nanomaterials, transition metal oxides, and electrically conducting polymers.

- **Carbon Nanomaterials** (Carbonaceous materials are popular among supercapacitors as an electrode material due to their accessibility, processing ability, large surface

area, low electrical resistivity, robust chemical environment, stability, and low cost. They offer energy storage capability through electric charges stored across the electrode/electrolyte interface. The average capacitance of carbon electrodes ranges from 50-200 F/g in aqueous, organic, and ionic electrolytes [23]. Carbon materials include activated carbons, nanotubes, graphene, CNFs, aerogels, mesoporous, and hierarchical carbons.)

- **Conducting Polymers** (Conducting polymers, such as polyaniline (PANI), poly (3,4-ethylenedioxythiophene), and polypyrrole, are electrode materials for Pseudocapacitors that deliver faradic charge. They have low electrical conductivity, low stability, and high cost compared to carbon materials. PANI is widely studied as a positive electrode due to its ease of synthesis and high capacitance [24]. Polypyrrole is gaining attention for its high capacitance, easy fabrication, and superior chemical and thermal stability in energy storage applications.)
- **Metal Oxides** (Metal oxides are widely used in storage devices, magnetic and optical, and electrochemical applications. Their surface interaction with target molecules is crucial. Nanoscale engineering of metal oxide increases surface area, improving electrochemical properties. Transition metal oxides like RuO₂, NiO, MnO₂, and Fe₂O₃ are popular for supercapacitors due to their Pseudocapacitive and EDLC properties. RuO₂ exhibits high specific capacitance and long cycling life, but its high cost and poor cycle life limit its commercial potential. MnO₂ is a potential material for energy storage and catalytic processes [25]. The other metal oxides that received considerable attention as an alternative electrode include BiFeO₃, Co₃O₄, Fe₃O₄, NiCo₂O₄ etc [26]

1.8.2 *Electrolyte*

The electrolyte plays a crucial role in facilitating the ionic conductivity within the supercapacitor. The capacitance of an EDLC relies on the electrolyte, which plays a crucial role in storing charge. The optimal ion and pore size is essential for optimal charge storage[27]. Poor electrolyte stability and chemical stability can increase resistance and reduce cycle life. Good electrolyte materials have low volatility, flammability, and

corrosion potential. ESs use four types of electrolytes: aqueous, organic, ionic liquids, and solid-state polymer electrolytes.

1.8.3 Separator

The separator is a porous material placed between the electrodes to prevent electrical short circuits while allowing ion flow. Important attributes of the separator include:

- **Porosity:** The separator should have high porosity to enable efficient ion transport, ensuring low internal resistance and high power density.
- **Mechanical Strength:** The separator should have sufficient mechanical strength to maintain its integrity during the charge/discharge cycles and prevent electrode contact.
- **Electrochemical Stability:** The separator should be chemically stable in the operating conditions of the supercapacitor, ensuring its long-term reliability.

1.9 Limitations for Supercapacitors

While supercapacitors offer many advantages, they also have some limitations that need to be considered. The main limitations of supercapacitors include:

- **Low Energy Density**
Supercapacitors have limited energy density, with commercially available electrochemical supercapacitors providing 3-4 Wh/kg. Heavy supercapacitors are necessary for large energy capacities, making low energy density a major disadvantage in short and medium-term applications [28]. This limitation restricts their application in devices requiring long-term energy storage, such as electric vehicles or grid-scale energy storage.
- **Costly**
The prices of production procedures and raw materials are crucial issues for supercapacitor technology. At this time, carbon and RuO₂ are often employed for practical applications. High surface area carbon compounds, however, are not costly. Few metal oxides (i.e. RuO₂) are highly expensive. Additionally, the electrolyte and

the separator may increase costs. While research and development efforts aim to reduce costs, widespread adoption may be hindered by the current cost constraints.

- **Self-Discharging**

Supercapacitors experience self-discharge over time, causing a gradual loss of stored energy. The rate of self-discharge is typically higher than that of batteries. Consequently, supercapacitors may not be suitable for applications that require long-term energy storage without frequent recharging. Also, Low duration and high self-discharging rate of supercapacitors (10–30% each day) have been cited as the main barrier to practical application [29].

- **Sensitive to Temperature**

Supercapacitors can be sensitive to temperature variations. Extreme temperatures can affect their performance and lifespan. High temperatures can accelerate degradation processes, leading to reduced capacitance and overall performance. Low temperatures can increase internal resistance, limiting the power output.

1.10 What is NiCo₂O₄

Nickel cobalt oxide (NiCo₂O₄) is a compound composed of nickel (Ni), cobalt (Co), and oxygen (O). It belongs to the family of transition metal oxides and exhibits interesting properties that make it useful in various applications. NiCo₂O₄ has an energy gap between 2.8 and 2.2 eV, an electrical resistivity of 62.4 n/m, and an electrical conductivity ranging from 0.05 to 10⁻⁶ S/cm. In supercapacitors, the NiCo₂O₄ has demonstrated remarkable conductivity performance [30]. Additionally, several studies have demonstrated that NiCo₂O₄ has a significantly lower electrical resistance than cobalt monoxide (CoO) and nickel oxide (NiO). The redox reactions provided by nickel cobalt oxide are thought to be richer than those of the monometallic nickel oxides and cobalt oxides because they incorporate contributions from both nickel and cobalt ions. More crucially, rich redox processes may be enabled by different nanostructures and diverse oxidation states for spinel nickel cobalt oxide to store more charges [31].

Table 1: Some of the major properties of NiCo₂O₄

Property	Description
Chemical composition	Nickel (Ni), Cobalt (Co), Oxygen (O)
Crystal structure	Spinel structure (Cubic)
Electrical conductivity	High~ 0.05 to 10 ⁻⁶ S/cm
Bandgap	2.8 and 2.2 eV
Catalytic activity	Exhibits catalytic activity, particularly (OER) and (ORR)
Density	5.98 Mg·m ⁻³
Molar Mass	240.5574 g/mol

1.10.1 Structure of NiCo₂O₄

The structure of nickel cobalt oxide is a spinel structure, which is a crystal arrangement where metal ions are distributed in a regular pattern. In this case, nickel and cobalt ions occupy some of the metal sites in the crystal lattice, while oxygen ions fill the gaps between them. This structure gives nickel cobalt oxide its unique properties.

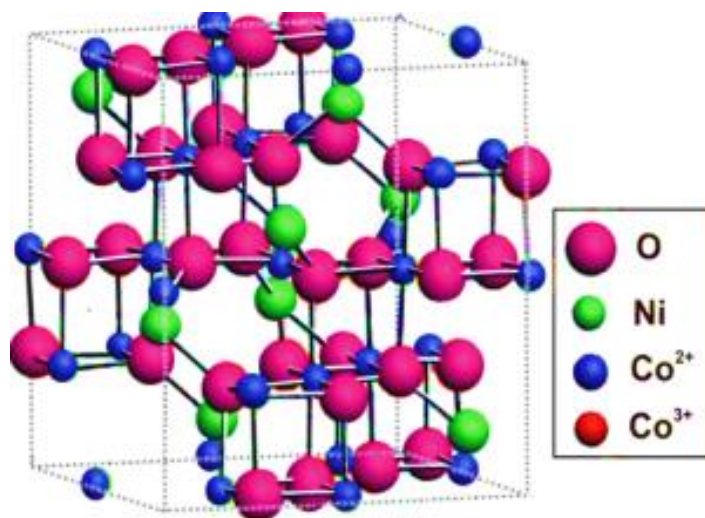


Figure 6: The Crystal structures of NiCo₂O₄ unit cell

NiCo₂O₄ crystal structure is depicted in Figure 6. NiO has a simple rock salt structure with octahedral Ni²⁺ and O²⁻ sites, while Co₃O₄ has a normal spinel structure with Co²⁺ ions in tetrahedral interstices and Co³⁺ ions in the octahedral interstices. Doping cobalt oxide with nickel increases electrical conductivity while maintaining the spinel structure. The generic spinel structure is formed from a face-centered cubic close packing of O²⁻ anions, with one-third of cations in the 2+ oxidation state and the remaining two-thirds as 3+ cations. The actual cation charge and size distribution are specific to the compound of interest [32]. The bulk structure of NiCo₂O₄ reveals nickel cations exclusively occupy octahedral sites, but charge distribution among nickel, cobalt, and tetrahedrons is challenging. Tetrahedral cations have an average metal-oxygen distance of 1.9182, while octahedral cations have a slightly greater distance of 1.9397. NiCo₂O₄ has higher electrical conductivity than monometallic nickel and cobalt oxides due to electron transport between cations with low activation energy in spinel cobalt oxide. Therefore, a variety of unique electrochemical characteristics are displayed by NiCo₂O₄. These characteristics relating to surface morphology and crystal structure are crucial for the NiCo₂O₄ electrode's electrochemical performance[33].

1.10.2 *Advantages and Disadvantages of NiCo₂O₄*

- **Advantages** (Due to its numerous benefits, including its high theoretical capacitance, environmental friendliness, low cost, and great abundance, ternary nickel cobalt oxide (NiCo₂O₄) has garnered a lot of attention among other metal oxides [34]. NiCo₂O₄ is noteworthy for having significantly better electrical conductivity and stronger electrochemical activity. NiCo₂O₄ also has magnetic characteristics as a result of the presence of transition metal ions and strong thermal stability, which allow it to maintain its structural integrity at high temperatures.)
- **Disadvantages** (Despite the many benefits that NiCo₂O₄ offers, several issues persist, demonstrating that the single NiCo₂O₄ structure exhibits constrained ion kinetics during redox reactions or is easily aggregated on the substrate, leading to low capacitance, unstable cycles, and poor charge-discharge performance [35]. Additionally, because the supercapacitor electrode inhibits the diffusion of the electrolyte, it will be challenging to electrochemically react with the bottom layer of NiCo₂O₄ active material on the substrate.)

1.11 What is SnS₂

SnS₂ refers to tin disulfide, which is a compound composed of tin (Sn) and sulfur (S). It is a member of the layered transition metal dichalcogenide (TMD) family, which includes various materials with a similar structure. The two accessible oxidation states of Sn, a heavier element in Group 14 of the Periodic Table, are divalent and tetravalent. Both Sn(II) and Sn(IV) compounds are recognized to exist, and there is a modest thermodynamic equilibrium between these two oxidation states. SnS₂ is a compound that only undergoes one oxidation state, and it has been suggested that SnS₂ is an n-type semiconductor. Furthermore, depending on how the materials were obtained and their polytype, the band gap of SnS₂ varies between 2.12 eV and 2.44 eV. SnS₂ exhibits high optical absorption coefficient $> 10^4$ cm⁻¹, n-type conductivity, and a moderately high charge carrier mobility of 18.3-230 cm²/V.s [36].

Table 2: Some of the major properties of SnS₂

Property	Description
Chemical composition	Tin (Sn), Sulfur (S)
Crystal structure	Layered structure (Rhombohedral)
Optical absorption coefficient	High~ > 10 ⁴ cm ⁻¹
Bandgap	2.12 eV and 2.44 eV
charge carrier mobility	18.3-230 cm ² /V.s
Density	4.5 g/cm ³
Molar Mass	182.81 g/mol
Melting Point	600 °C (1,112 °F; 873 K)

1.11.1 Structure of SnS₂

The structure of SnS₂ consists of layers of Sn atoms sandwiched between layers of S atoms. Each Sn atom is covalently bonded to two S atoms in trigonal prismatic coordination, while each S atom is bonded to three Sn atoms. The layers are held together by weak van der Waals forces, allowing them to slide past each other.

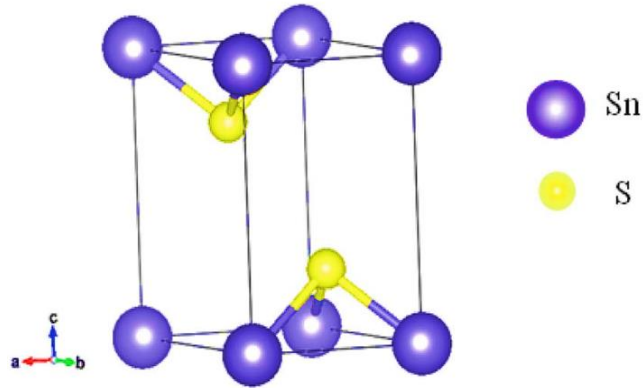


Figure 7: The Crystal structures of SnS₂

Here figure 7 shows the crystal structure of SnS₂, which demonstrates that each Sn atom is octahedrally surrounded by six S atoms because Sn is wedged between two planes of S inside one plane [37]. Each unit cell has three atoms. A Tri layer made of S-Sn-S atoms is held together by van der Waals forces along the c-axis and internal covalent bonds in the ab plane. Therefore, such layered structure gives rise to unique properties, including anisotropic electrical conductivity and mechanical flexibility.

1.11.2 Advantages and Disadvantages of SnS₂

- **Advantages** (The advantages of SnS₂ include its non-toxicity, high energy density, and extended cycle life in energy storage technologies, as well as the affordability and Earth-abundance of its component components (Sn and S). SnS₂ is also a semiconductor material with a direct bandgap, enabling effective light absorption and emission [38].)
- **Disadvantages** (SnS₂ can undergo degradation or chemical reactions in certain environments, particularly under highly oxidative or corrosive conditions. This limited stability may restrict its use in applications that require long-term durability [39]. Additionally, SnS₂ can undergo degradation or chemical reactions in certain environments, particularly under highly oxidative or corrosive conditions. This limited stability may restrict its use in applications that require long-term durability.)

1.12 Significance and Research Objectives Major Revision

The primary objective of this research is to evaluate the performance of NiCo₂O₄@SnS₂/CC composite in a supercapacitor. Supercapacitors are gaining acceptance even though they are still regarded as developing technologies that need more work to overcome their drawbacks. Because supercapacitors require a lot of protection and are expensive, researchers have been pushed to employ a variety of innovative materials as electrodes in them. This point of view claims that the study is important since it provides superior data on whether the integration of NiCo₂O₄@SnS₂/CC composite improves the rate performance of supercapacitors.

1.12.1 *Research Objectives*

- Synthesizing the NiCo₂O₄@SnS₂/CC electrode material for supercapacitors.
- Characterization of the synthesized NiCo₂O₄@SnS₂/CC electrode.
- Device testing of NiCo₂O₄@SnS₂/CC electrode as a supercapacitor.
- Examining the uses of supercapacitors with composite NiCo₂O₄ and SnS₂ electrodes and putting these nanostructures to use in applications associated with energy.

CHAPTER 2: LITERATURE REVIEW

2.1 Historical Background

The global economy's rapid growth has led to a need for alternative, environmentally friendly energy sources to reduce reliance on fossil fuels. Storage and conversion technologies have been developed to address this demand. However, renewable energy sources have sporadic characteristics that can be altered by environmental factors. Despite advancements in harvesting technologies like fuel cells, lithium-ion batteries, and dye-sensitized solar cells, more suitable methods for absorbing and storing generated energy are still needed[40]. Due to their intriguing characteristics, such as high-power densities, lengthy cycling lifetimes, and quick charge/discharge processes, supercapacitors, also known as electrochemical capacitors, have recently undergone extensive research to serve as one of the most promising candidates for next-generation energy storage devices, as evidenced by the number of literature displayed in Figure 8 [41].

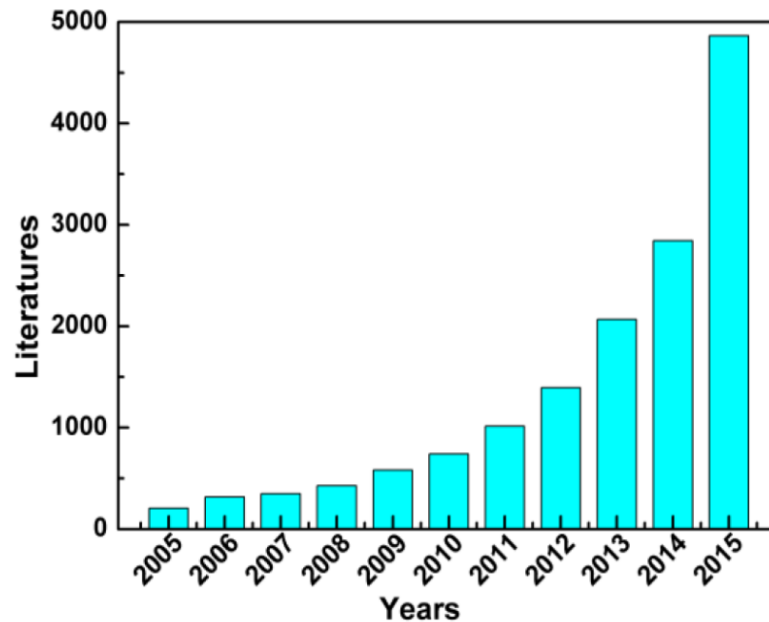


Figure 8: The numbers of reported literature related to supercapacitors from 2005 to 2015

2.2 Supercapacitors

Advanced technologies and miniaturized electronic devices require rechargeable energy storage. Li and Li-ion batteries were discovered in the late 1990s, but their finite life makes maintenance and replacement difficult. Electrochemical capacitors (ECs), also known as supercapacitors, store energy at the interface between a porous electrode and an electrolyte through ion accumulation. These capacitive supercapacitors provide fast charge/discharge rates, and high power, and can sustain millions of cycles with reasonable power density. Micro-scale supercapacitors can satisfy various micro-power demands and replace micro-batteries in electrical energy storage applications where high-power delivery is required in a short time [42].

2.2.1 Types of Supercapacitors

The supercapacitor's functioning idea is based on the distribution of ions from the electrolyte to the electrode surface area, as well as energy storage. Supercapacitors are classified into three types based on how they store energy: pseudo capacitors, hybrid supercapacitors, and electrochemical double-layer capacitors.

2.2.2 Electrical Double Layer Capacitor

EDLCs (store charge electrostatically) have a charge storage mechanism based on charge separation at the interface between an electrolyte and an electrode, resulting in long cyclic lives and higher energy density due to the double layer and reduced electrode distances. Unlike batteries, EDLCs can withstand millions of cycles but are best for a few thousand cycles [43], [44].

2.2.3 Pseudo capacitors

The working mechanism for Pseudo pseudo-capacitors is based on faradic redox reactions, its electrode materials are based on conductive polymers, metal oxides or metal-doped

carbons. When a potential is applied to a pseudo capacitor reduction and oxidation takes place on the electrode material, which involves the passage of charge across the double layer, resulting in faradic current passing through the supercapacitor cell. The faradic process involved in pseudo capacitors allows them to achieve greater specific capacitance and energy densities compared to EDLCs. These supercapacitors have higher energy density due to the electrode material. These supercapacitors have higher energy density as compared to electrochemical layer double-layer capacitors, but their cyclic lives are shorter [45].

2.2.4 Hybrid Capacitors

These supercapacitors incorporate mechanisms from both pseudo-capacitors and EDLCs. A supercapacitor consists of two electrodes separated by a semipermeable membrane which acts as a separator to isolate from electrical contact. An electrolyte solution is impregnated on the electrodes and separator, which enables the flow of ions between electrodes and prevents electronic current from discharging the cell [46].

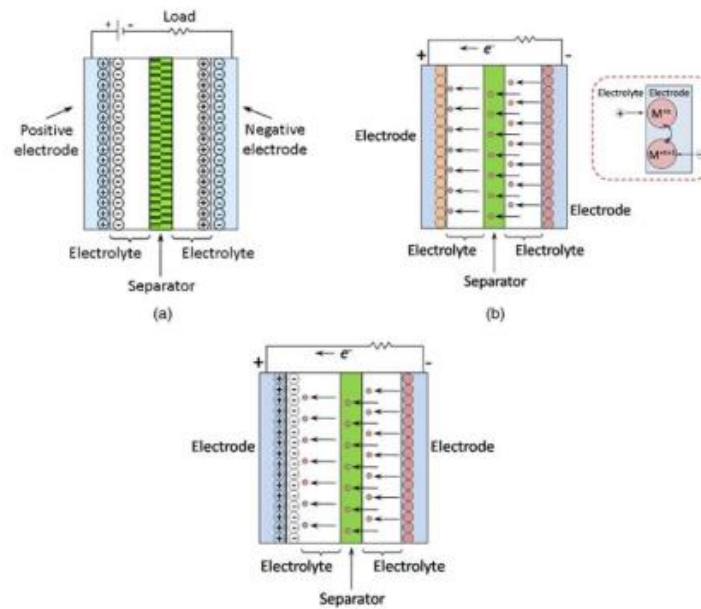


Figure 9: Schematic representation of three types of Supercapacitor (a) EDLCs (b) Pseudo capacitor (c) Hybrid Capacitor. Copyright 2018 by American Society of Civil Engineers

2.2.5 Composite Hybrid

Composite electrodes combine carbon-based materials with either conducting polymer or metal oxides in a single electrode, due to this we can say that a single electrode will have both physical as well as chemical charge storage mechanisms. Carbon-based materials have a capacitive double-layer of charge and high specific surface area due to which the contact between pseudocapacitive materials and electrolytes increase. Due to the Faradic reaction, pseudocapacitive material increases capacitance in composite hybrid electrodes [47].

There are two different types of composite hybrid capacitor:

1. Binary composites
2. Ternary composites

In binary composites, two different electrode materials are involved, while in ternary composites three different electrode materials are used to form a single electrode.

2.2.6 Asymmetric Hybrid

In asymmetric hybrids, non-faradic and faradic processes work by coupling and EDLC with a pseudo capacitor electrode. They are set in this way that for negative electrode carbon material is used while for positive electrode either metal oxide or conducting polymers are used.

2.2.7 Battery Type Hybrid

In battery type hybrid, two different electrodes are combined same as asymmetric hybrids, but in this case, they are made by combining a battery electrode with supercapacitor electrode. This type of capacitor is formed to use the properties of both supercapacitors and batteries.

2.3 Common Electrode Materials used in supercapacitor

The parameters that depend on the type of electrode materials used in supercapacitors are charge storage and capacitance.

2.3.1 Carbon Materials used in supercapacitor

For the fabrication of supercapacitor carbon and different types of carbon materials are mostly used. There are following reasons due to which we use carbon and its various types:

1. High surface area
2. Low cost
3. Availability
4. It has established electrode production technologies

The charge storage mechanism used by carbon type materials is electrochemical double layer which is between the electrode and electrolyte. Due to this the capacitance mostly relies on the surface area available to electrolyte ions. The important factors that effects the electrochemical performance are [48]:

1. Specific surface area
2. Pore shape and structure
3. Pore size distribution
4. Surface functionality
5. Electrical conductivity

The carbon materials used as electrode materials are [49]:

- Activated carbon

- Carbon aerogels
- Carbon nanotubes
- Graphene

2.3.1.1 Activated Carbon

The most commonly used electrode material is activated carbon (AC) because it has a large surface area, good electrical properties and reasonable cost [58]. AC can be produced by the activation of different types of carbon materials either by physical or chemical means (e.g. wood, coal nutshell etc.). In physical activation process the treatment of carbon precursors at a high temperature (700-1200°C) in the presence of oxidizing gases like air, CO₂ and steam is involved. In chemical activation case, it is carried out at a lower temperature (400-700°C) using activating agents such as phosphoric acid, sodium hydroxide, potassium hydroxide, and zinc chloride [50].

2.3.1.2 Carbon Nanotube

After the discovery of CNT very significant developments took place in the field of science and technology of carbon materials. In a supercapacitor the resistance of the components is the main factor which tells about the power density. CNT get great attention as an electrode material for the application of supercapacitor due to its unique properties like porous structure, good thermal, mechanical and electrical properties [51], [52]. CNTs are produced by catalytic decomposition of hydrocarbons and by carefully using different parameters, it becomes possible to produce nano structures in different conformations and in controlled crystalline structure. CNT, unlike other different carbon-based electrodes, has mesopores that are interconnected. This property gives a continuous charge distribution which uses all the reachable surface area.

2.3.1.3 Graphene

Recently graphene has been significant attention in research as well as in industrial areas. Graphene is a 2D layer structure of unique carbon material which has great potential for energy storage device applications like supercapacitor because of its unique characteristics

of very high electrical conductivity, large surface area and chemical stability [53]. Recently, graphene is most extensively used in supercapacitor application because when graphene is used as electrode material of supercapacitor it does not depend on the pore's distribution at solid state, unlike other carbon materials such as ACs and CNTs etc [54].

2.3.2 Metal Oxide

Metal oxides are other alternative materials used in electrodes fabrication materials for supercapacitor application because they have high specific capacitance and low resistance, which makes it easier to form supercapacitors with high energy and power. The commonly used metal oxides for supercapacitor application are following [55]:

1. Nickel oxide (NiO)
2. Ruthenium dioxide (RuO₂)
3. Manganese oxide (MnO₂)
4. Iridium oxide (IrO₂)

Metal oxide production cost is lower, and it uses milder electrolytes which make it a suitable alternative.

2.3.3 Conducting Polymers

Conducting polymers have been extensively using as electrode material for supercapacitor applications because they can be easily produced and have low cost [55]. Conducting polymers have a high capacitance and conductivity value as compared to other electrodes that are formed of carbon. The conducting polymers can be used in different electrode configurations such as, the n/p type configuration, in this configuration n doped is negatively charged and p doped is positively charged electrodes are used which gives a high energy and densities.

2.3.4 Composites

Hybrid-type supercapacitors mostly use composite materials. Composite materials contain combinations of different carbon materials with either conducting polymers or metal oxides, therefore they have properties of both EDLC and pseudo-capacitor materials. Electrodes for supercapacitors made of CNT and polypyrrole mixtures exhibit higher capacitance values to electrodes that are either based on CNTs or polypyrrole [56].

2.4 Why Oxides and Sulphides as an Electrode Material

Oxides and sulfides are commonly used as electrode materials for supercapacitors due to their unique properties that make them suitable for energy storage applications. Supercapacitors, also known as electrochemical capacitors or ultracapacitors, are energy storage devices that store and release energy through electrostatic charge separation at the interface of an electrode and an electrolyte. Here are some reasons why oxides and sulfides are favored as electrode materials for supercapacitors:

- **High Specific Capacitance**

Oxides and sulfides often exhibit high specific capacitance, which is a measure of the amount of charge a material can store per unit mass or surface area. This high specific capacitance allows for the efficient storage of electrical energy in supercapacitors.

- **Conductivity**

Many oxides and sulfides possess good electrical conductivity, which is crucial for the rapid movement of ions within the electrode material. Higher conductivity facilitates faster charge and discharge rates, improving the overall performance of supercapacitors.

- **Chemical Stability**

Oxides and sulfides are often chemically stable in the presence of electrolytes used in supercapacitors. This stability is essential for the long-term reliability and durability of the supercapacitor

- **Abundance and Low Cost**

Some oxide and sulfide materials are abundant and cost-effective, making them attractive for large-scale production of supercapacitors. This is particularly important for the commercial viability of energy storage technologies.

- **Tunable Properties**

The properties of oxides and sulfides can be tailored by modifying their composition, structure, or morphology. This tunability allows researchers to optimize the material for specific performance requirements, such as high energy density, long cycle life, or environmental considerations.

Nanostructured Ni/Co oxides/hydroxides are considered attractive electrode materials for supercapacitors due to their high theoretical specific capacitances (e.g., 3750 F/g for NiO and 3560 F/g for Co₃O₄), cheap cost, and ecological compatibility [57]. Charge storage in Ni/Co oxides/hydroxides occurs through reversible redox between Ni²⁺/Ni³⁺ or Co²⁺/Co³⁺ states in alkaline electrolytes [58]. Nanostructures, including nanowires, nanosheets, nanoflowers, and nanobelts, improve supercapacitor performance by increasing surface area and shortening ion diffusion and transport paths.

Vijayakumar et al. synthesized NiO using microwave heating at various calcination temperatures [59]. Calcinating NiO at 300°C resulted in a nanoflake structure and a maximum

The specific capacitance is 401 F/g at 0.5 mA cm⁻². **Yuan et al.** created mesoporous Co₃O₄ nanosheet arrays on a Ni foam substrate, resulting in rapid ion and electron transport and high specific capacitance of 2735 F/g at 2 A/g with little degradation after 3000 cycles [60]. **Hu et al.** examined the supercapacitor performance of Ni(OH)₂ and Co(OH)₂ films made using a simple electrodeposition approach [61]. Ni(OH)₂ has a greater specific capacitance than Co(OH)₂ (2217 F/g against 549 F/g at 1.0 mA cm⁻²), Co(OH)₂ demonstrated higher rate capability and energy efficiency.

Despite having high specific capacitances, Ni or Co oxides/hydroxides have poor rate capability and cycle stability due to limited conductivity and substantial volume changes

during charging and discharging [62]. Lu et al. created Ni(OH)₂ nano wall films that had a high specific capacitance of 2675 F/g at 5 mA cm⁻². However, when the current density was raised to 30 mA cm⁻², the specific capacitance decreased significantly to 1150 F/g [63]. Composite materials with carbon are commonly used to increase electrochemical performance and address concerns.

Metal sulphides offer greater electrical conductivity, thermal stability, and redox chemistry than oxides, making them ideal electrode materials for supercapacitors. Metal sulphides, including MnS, VS₂, FeS₂, CuS, SnS₂ and WS₂, have been studied as electrode materials for supercapacitors. **Mahboob et al.** concluded that Tin (IV) sulphide, known for its layered structure, can efficiently generate two-dimensional morphologies. Its availability, non-toxicity, and cost-effectiveness make it an attractive electrode material. Tin (IV) sulfide's faradic behaviour makes it an ideal material for supercapacitor applications [64].

2.5 Binary Metal Oxides

Binary metal oxides, including NiCo₂O₄, ZnCo₂O₄, CoFe₂O₄, NiMoO₄, CoMoO₄, MnMoO₄, and, FeMoO₄ have gained popularity as electrode materials for supercapacitors in recent years [65]. Binary metal oxides outperform unitary metal oxides in electrochemical performance due to the synergistic impact and capacitive contribution of individual components [66]. **Wang, Qiufan, et al.** a simple hydrothermal approach produced urchin-like NiCo₂O₄ nanorods with a high specific capacitance of 1650 F/g at 1 A/g and 9.2% capacitance loss after 2000 cycles at a high charged-discharge rate of 8 A/g [67]. **Guo et al.** created a binder-free electrode by growing NiMoO₄ nanowires on flexible carbon fabric. They achieved a high specific capacitance of 1587 F/g at 6.25 A/g [68]. However, the quick charge/discharge process caused structural deformation, resulting in only 76.9% capacitance retention after 4000 cycles.

Table 3: NiCo₂O₄ and SnS₂ based nanostructures.

Title	Year	Author/Journal	Conclusion
<p>Binary Nickel-Cobalt Oxides Electrode Materials for High-Performance Supercapacitors: Influence of its Composition and Porous Nature</p>	<p>2015</p>	<p>J. Zhang et al., (2015) /ACS Applied Materials and Interfaces.</p>	<p>The binary metal oxide with the precise molar ratio of Ni:Co = 0.8:1 annealed at 300 °C has an optimal specific capacitance of 750 F/g, a high energy density of 34.9 Wh/kg at a power density of 875 W/kg, and a long cycling life (86.4% retention of the starting value after 10,000 cycles).</p>
<p>Capacitive performance of electrochemically deposited Co/Ni oxides/hydroxides on polythiophene-coated carbon-cloth</p>	<p>2021</p>	<p>Gülten Atun et al., (2021) / Journal of Polymer Engineering.</p>	<p>Co, Ni, and Co-Ni hydroxide-coated PTh electrodes had capacitances of 100, 569, and 221 F/g at 5 mA/cm² in 1 M KOH, respectively.</p>

<p>Mesoporous NiCo₂O₄ nanoneedles grown on three dimensional graphene networks as binder-free electrode for high-performance lithium-ion batteries and supercapacitors</p>	<p>2015</p>	<p>Sainan et al., (2015) /Electrochimica Acta.</p>	<p>The hybrid has long-term cycling stability up to 2000 cycles for LIBs and a high specific capacitance of 970 F g⁻¹ at 20 A g⁻¹ for SCs. It also retains capacitance at ~96.5% after 3000 cycles.</p>
<p>Tin-based metal-phosphine complexes nanoparticles as long-cycle life electrodes for high-performance hybrid supercapacitors</p>	<p>2022</p>	<p>Chengyu et al., (2022) /Journal of Colloid and Interface Science</p>	<p>At a current density of 1 A g⁻¹ in 6 M KOH, [Sn(OH)₄(PPh₃)₂] and [Sn(OH)₂(PPh₃)₂] may reach specific capacitances of 1204F g⁻¹ and 764F g⁻¹, respectively.</p>

<p>Hierarchical porous NiCo₂O₄ nanowires for high-rate supercapacitors</p>	<p>2012</p>	<p>Hao et al., (2012) /Chemical Communications.</p>	<p>Nickel cobalt oxide nanowires have a high specific capacitance of 743 F g⁻¹ at 1 A g⁻¹), outstanding rate performance (78.6% capacity retention at 40 A g⁻¹), and cycling stability (only 6.2% loss after 3000 cycles).</p>
<p>Hierarchical NiCo₂O₄ nanosheets@hollow microrod arrays for high-performance asymmetric supercapacitors</p>	<p>2014</p>	<p>Xue-Feng Lu et al., (2014)/ Journal of Materials Chemistry.</p>	<p>NiCo₂O₄ NSs@HMRA electrodes have a high specific capacitance (C_{sp}) (678 F g⁻¹ at 6 A g⁻¹) and excellent cycle stability (96.06% retention after 1500 cycles).</p>
<p>Characterization of nanostructured nickel cobalt oxide-polyvinyl alcohol</p>		<p>Siwatch, P et al.,(2021)/ Journal</p>	<p>NCO-PVA films as the electrodes, exhibits the specific capacitance value of</p>

<p>composite films for supercapacitor application.</p>	<p>2021</p>	<p>of Alloys and Compounds.</p>	<p>50 F g⁻¹ and energy density of 18.9 W h kg⁻¹.</p>
<p>Hierarchical nickel–cobalt oxide and glucose-based carbon electrodes for asymmetric supercapacitor with high energy density</p>	<p>2020</p>	<p>Erusappan, E et al.,(2020)/ Journal of the Taiwan Institute of Chemical Engineers.</p>	<p>Ni-Co oxide and glucose-based carbon electrode shows Energy density of 45.3 Wh kg⁻¹ was achieved at a power density of 0.743 kW kg⁻¹ (1 A g⁻¹) and the supercapacitor showed excellent cycling stability of 89.7% over 10,000 cycles.</p>

CHAPTER 3: EXPERIMENTAL WORK

The synthesis processes for pure NiCo_2O_4 and the $\text{NiCo}_2\text{O}_4@\text{SnS}_2$ composite on carbon cloth are covered in depth in this chapter, which is followed by the fabrication of both electrodes for a supercapacitor.

3.1 Reagents and materials

From Daejung Chemicals, sulfuric and phosphoric acids ($\text{H}_2\text{SO}_4/\text{H}_3\text{PO}_4$) were acquired. MERCK (E. MERCK, Darmstadt, F. R. Germany) provided the nickel nitrate hexahydrate $\text{Ni}(\text{NO}_3)_2 \cdot 6\text{H}_2\text{O}$, sodium hydroxide pellets (NaOH), and potassium manganate (KMnO_4), while Sinopharm Chemical Reagent Co. provided the urea. From Scharlau (Spain), we obtained ethanol (99.8%), glucose, isopropanol, and cobalt nitrate hexahydrate $\text{Co}(\text{NO}_3)_2 \cdot 6\text{H}_2\text{O}$. Thioacetamide and tin chloride pentahydrate ($\text{SnCl}_4 \cdot 5\text{H}_2\text{O}$) were provided by Duksan Pure Chemicals Co. Ltd. All of the reagents were purchased, utilized in experiments without additional purification, and were accessible at commercial scale. There was also usage of deionized water. The substrate utilized was Carbon Cloth.

3.2 Synthesis of Materials

A two-step hydrothermal approach was used to manufacture the integrated electrode $\text{NiCo}_2\text{O}_4@\text{SnS}_2/\text{CC}$ along with Modified Hummers Method for the activation of carbon cloth. Firstly, pure NiCo_2O_4 was synthesized and deposited on carbon cloth as reported in [69]. Secondly, $\text{NiCo}_2\text{O}_4/\text{CC}$ electrode was further utilized to deposit SnS_2 as reported in [70]. As a result, two electrodes $\text{NiCo}_2\text{O}_4@\text{SnS}_2/\text{CC}$ and $\text{NiCo}_2\text{O}_4/\text{CC}$ were formed for further investigations.

3.2.1 Treatment on Carbon-Cloth

Every reagent utilized was of analytical grade from without any further purification. Firstly, in order to give CC a hydrophilic surface, CC was treated using an enhanced Hummer's technique in a solution of $\text{H}_3\text{PO}_4/\text{H}_2\text{SO}_4$ with a volume ratio of 1:5, 0.25 g of

KMnO₄, and 20 ml of DI water. Under 50 °C, the sonication process took place in 15 minutes. The pretreated CC was obtained after ethanol and DI water rinsing.

3.2.2 Preparation of NiCo₂O₄ nanostructures

NiCo₂O₄/CC was simply prepared by following method:

- In a two-step technique firstly, a clear pink solution was created by stirring 2 mmol Co(NO₃)₂·6H₂O, 1 mmol Ni(NO₃)₂·6H₂O, and 5 mmol urea in 50 ml of distilled water and 5 ml of ethanol for 30 minutes.
- A piece of a pretreatment carbon cloth and the prepared pink solution were placed in a 50 ml Teflon-lined stainless-steel autoclave.
- At 120 °C, the hydrothermal process took 16 hours to complete.
- The coated carbon cloth was cleaned with deionized water and ethanol and then dried at 60 °C in an oven.
- As a result, NiCo₂O₄/CC nanostructures were generated on the carbon fabric using a straightforward hydrothermal technique.



Figure 10: Preparation of NiCo₂O₄ nanostructures

3.2.3 Preparation of NiCo₂O₄@SnS₂ nanostructures

Furthermore, NiCo₂O₄@SnS₂/CC was prepared by second hydrothermal method:

- The $\text{NiCo}_2\text{O}_4@\text{SnS}_2/\text{CC}$ integrated electrode was made by growing SnS_2 nanostructures on the NiCo_2O_4 matrix using a subsequent hydrothermal procedure.
- In a 50 ml Teflon-lined stainless-steel autoclave holding the already prepared NiCo_2O_4 nanostructures on carbon cloth.
- The solution of 1 mmol $\text{SnCl}_4 \cdot 5\text{H}_2\text{O}$ and 2 mmol thioacetamide was prepared, magnetically stirred for 30 min., and then heated at 160°C for 16 h.
- The sample was thereafter taken out of the heating oven and repeatedly washed in ethanol and deionized water before being dried in a 60°C oven.
- Therefore, a practical method was successfully used to manufacture the integrated electrode $\text{NiCo}_2\text{O}_4@\text{SnS}_2/\text{CC}$.

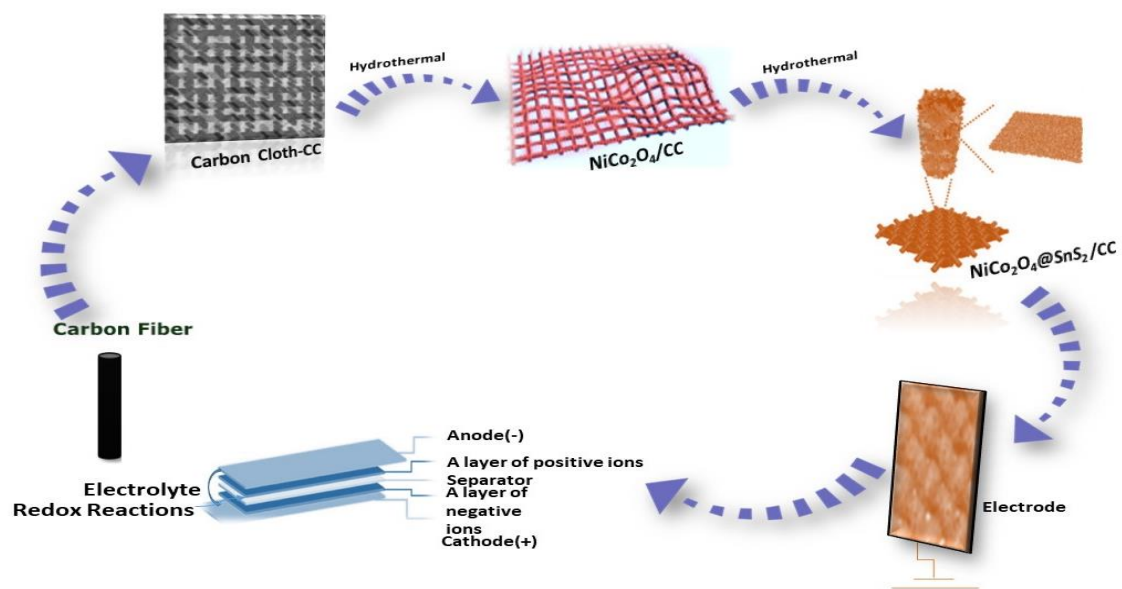


Figure 11: Preparation of $\text{NiCo}_2\text{O}_4@\text{SnS}_2/\text{CC}$ nanostructures

3.2.4 Fabrication of Working Electrode

Three to four pieces of the NiCo_2O_4 and SnS_2 nanostructure-grown on carbon fabric were cut out for various measurements. $\text{NiCo}_2\text{O}_4/\text{CC}$ and $\text{NiCo}_2\text{O}_4@\text{SnS}_2/\text{CC}$ nanostructures having active surface areas of 0.25 cm^2 and 1.5 mg of mass load, respectively, were used to create the working electrode.

CHAPTER 4: CHARACTERIZATION TECHNIQUES

4.1 Instrumentation and Measurements

The elemental composition, phase information, and crystal structure were assessed using X-ray diffraction, a Bruker Model D8 Advance x-ray powder diffractometer (XRD) with x-rays from a Cu-K source ($\lambda=1.5418$). The surface morphology was examined using an energy dispersive spectrometer (EDS) and a field emission scanning electron microscope (FESEM, TESCAN MIRA-3). Using the Horbia Xplora spectrometer (laser wavelength: 532 nm), a Raman spectrum was acquired. A Nicolet iS50 FTIR spectrometer is used to record the spectra using FTIR, or Fourier-transform infrared spectroscopy. High-resolution transmission electron microscopy (HRTEM, JEOL-JEM-201, 200 kV) was used for the detailed structural evaluation. At Electra, X-ray photoelectron spectroscopy (XPS) measurements were performed using a Super ESCA beam. Electrochemical measurements like cyclic voltammogram (CV), Galvanic charge-discharge (GCD) and Electrochemical impedance spectroscopy (EIS) were carried out utilizing a three-electrode setup and an electrochemical workstation (CH1660C) with 3M KOH solution as the electrolyte.

4.2 Raman Spectroscopy

Raman spectroscopy is an effective technique for characterizing and identifying many types of materials, including solids, liquids, and gases. It is a method that provides information on a material's molecular vibrational modes without touching, harming, or invading it. The Raman technique is based on the inelastic scattering of light by a material. When a photon of light interacts with a molecule, it may stimulate the molecule to a higher vibrational state. By emitting a light photon with a different energy, the molecule relaxes back to its ground state during the Raman shift process.

When a molecule scatters light, the oscillating electromagnetic field of the photon causes the molecular electron cloud to become polarised, which elevates the molecule's energy and transfers the photon's energy to it. This is the development of a very short-lived

complex between the photon and the molecule, which is generally referred to as the virtual state of the molecule. Since the virtual state is unstable, the photon is quickly reemitted as scattered light. A spectrometer is used to collect and analyses the scattered light in the Raman technique, which includes shining a laser beam of a certain wavelength on the sample. Surface-enhanced Raman scattering (SERS) and resonance Raman scattering (RRS) are two techniques that can be used to improve the signal of the generally weak Raman scattered light.

4.2.1 Working Principle

The Raman effect arises from the interaction of light with matter. When a monochromatic (single wavelength) light beam, typically from a laser, is directed onto a sample, two types of light scattering can occur:

- **Rayleigh Scattering:** The vast majority of scattered light remains at the same wavelength (frequency) as the incident light. This is known as Rayleigh scattering and does not provide much useful information for Raman spectroscopy.
- **Raman Scattering:** A small fraction of the incident light undergoes a change in frequency due to interactions with the sample's molecules. This process is called Raman scattering, and it results in the scattered light having either a lower or higher frequency compared to the incident light. The shift in frequency corresponds to the vibrational energy levels of the molecules in the sample.

The energy difference between the incident and scattered light is related to the vibrational and rotational energy levels of the molecules in the sample. By analyzing the frequency shifts in the Raman-scattered light, researchers can determine the vibrational modes and rotational states of the molecules, providing valuable information about the sample's molecular structure and composition.

There are two main types of Raman scattering:

- **Stokes Raman Scattering:** In this type, the scattered light has lower frequency (longer wavelength) than the incident light. It occurs when the incident photons transfer energy to the molecules, exciting them to higher vibrational states.
- **Anti-Stokes Raman Scattering:** In this type, the scattered light has higher frequency (shorter wavelength) than the incident light. It occurs when the molecules in the sample lose energy by emitting a photon during the scattering process, leading to a transition to lower vibrational states.

The Raman scattered light is collected and analyzed using a spectrometer, which separates the different frequencies of light, allowing researchers to obtain a Raman spectrum. The Raman spectrum provides a unique fingerprint of the sample's molecular composition, helping to identify chemical compounds and study molecular interactions. In summary, the working principle of Raman spectroscopy involves shining a laser light on a sample, measuring the frequency shifts in the scattered light, and analyzing the resulting Raman spectrum to gain insights into the molecular structure and composition of the sample.

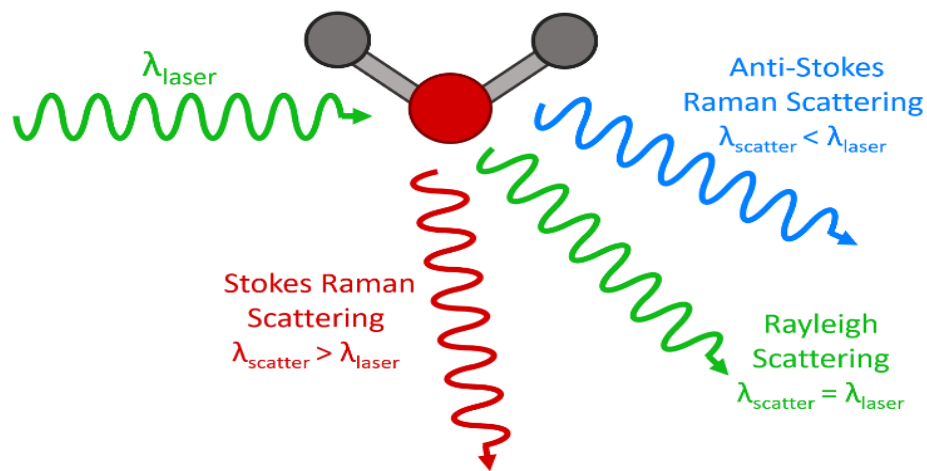


Figure 12: Three types of scattering processes

4.3 XRD (X-ray diffraction)

X-ray diffraction spectroscopy is a powerful analytical technique used to study the atomic and molecular structure of materials. It is based on the principles of X-ray diffraction, which was first observed by the physicist Max von Laue in 1912 and further developed by William Henry Bragg and his son William Lawrence Bragg. It gives information about strains; defects in crystal structure as well as average particle size of crystal can also be calculated by using this. Diffraction analysis is done in this technique. When two wavelengths of same frequency and amplitude pass through a medium in this way the crest and trough superimpose on each other, and amplitude of the wave maximizes it leads to formation of constructive interference. But if two waves pass through the sample in such way that crest falls on trough that subtract the influence of each other and resultant destructive interference has minimum amplitude. There are three methods for the analysis of crystal structure i.e.,

- Laue Method
- Powder X-ray diffraction
- Rotating crystal structure

Powder x-ray diffraction analysis is the most advanced and most commonly used method especially for the characterization of nanomaterials. The crystallite size of nanoparticles in powder x-ray diffraction analysis is done by using two methods i.e.

- Debye Scherrer Method
- Diffractometer Method

The sample used in powder XRD analysis is finally grinded along with Molybdenum or copper as reference materials.

4.3.1 Working Principle

XRD is regulated by an equation known as Bragg's Law. When X-rays are dispersed from a crystalline material, the measured angles of constructive interference are proportional to its lattice spacing. Bragg's law states that when a monochromatic x-ray of wavelength λ interacts with a regular array of atoms on the surface of a crystalline material at an incidence angle θ , it scatters light. Bragg's equation describes the conditions that allow for constructive interference.

$$2d\sin\theta = n\lambda$$

Where n is the integer, $n =$ order of interference

d is the lattice spacing of the crystal

$\theta =$ angle of incidence of x-ray beam

Reflection from the crystal appears when the

incident angle satisfies the condition $\sin\theta = n\lambda/2d$.

X-ray diffraction machines consist of three basic components i.e.

- Source of X-rays or x-ray tube
- Sample holder
- Detector

The X-rays are produced by heating a filament which produces the electrons in cathode ray tube. These electrons are then bombarded on the target material i.e., copper or molybdenum. The targeting electrons have enough energy to penetrate the crystal structure and excite inner shell electrons. The acceleration and deceleration of these electrons produce waves in X-ray region. These X-rays are then directed on to the sample in the sample chamber.

When the incident angle of X-rays matches the reflected angle between the planes of crystal constructive interference occurs and it is recorded by the detector. The data obtained by X-

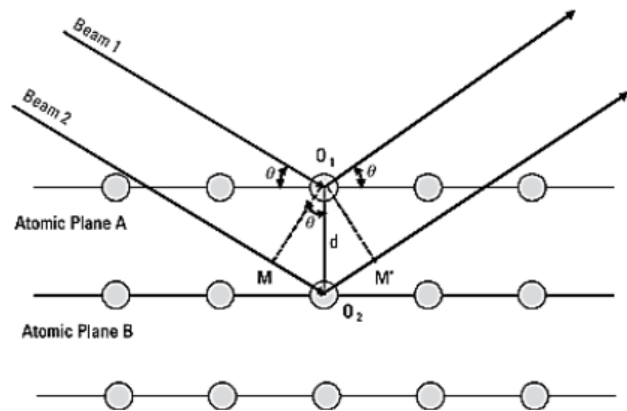


Figure 13: X-ray diffraction by planes of crystal

ray diffraction analysis can be used for the measurement of lattice constant of unit cell of crystal, Crystallite size, samples material density and pore fraction. The following are the formulas used for the calculations of all above-described values.

For the calculation of Lattice Constant of unit cell of sample material formula is:

$$a = \frac{\lambda (h^2 + k^2 + l^2)^{1/2}}{2 \sin \theta}$$

Where, a = wavelength of X-ray

hkl = miller indices

θ = is diffraction angle

Formula used for the measurement of crystallite size.

is Debye Scherrer formula.

$$t = \frac{0.9 \lambda}{\beta \cos \theta}$$

Where, θ = diffraction angle

λ = Wavelength of X-ray used for analysis

β = is full width half maximum (FWHM)

In summary, X-ray diffraction is a technique specifically used to study the atomic arrangement in crystalline materials, while X-ray spectroscopy encompasses various methods to analyze the properties and composition of materials using X-rays.

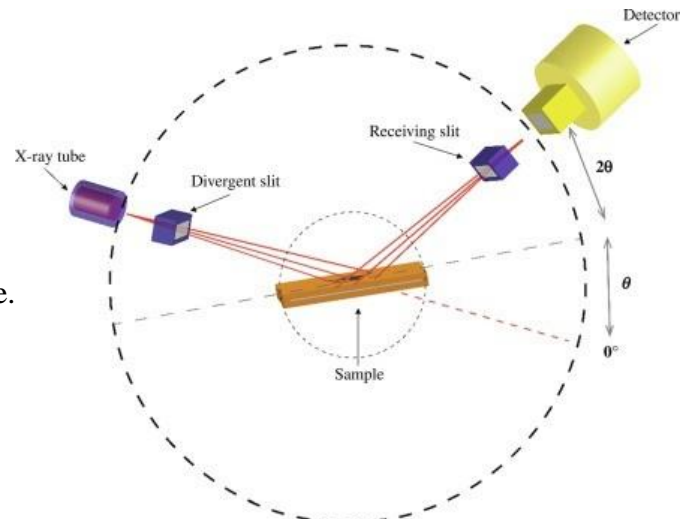


Figure 14: X-ray diffraction Schematic

4.4 SEM (Scanning Electron Microscopy)

In scanning electron microscope, the interaction of electrons with matter is studied to find the topography, composition, particles size and phase mapping of the nano or bulk material. When a high energy electron beam strikes a material, many interactions occur between them which can be used for the analysis of sample. When electrons in the beam interact with atoms on the sample's surface, they emit a variety of signals, such as characteristic X-rays, back-scattered electrons, secondary electrons, light cathodoluminescence, transmitted electrons, and absorbed current (specimen current), all of which reveal information about the sample's composition and topography. Secondary and backscattered electrons are the most typical signals utilised to image samples. Secondary electrons provide information on sample topography and morphology, whereas backscattered electrons indicate the composition of multiphase materials.

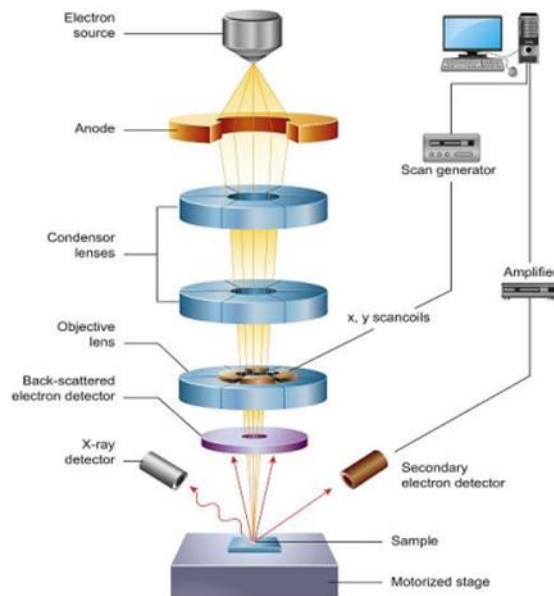


Figure 15: Illustration of SEM

4.4.1 Working Principle

The working principle of SEM involves several key steps:

- **Electron Source:** SEM uses a high-energy electron source, typically a tungsten filament or a field emission gun (FEG), to generate a beam of electrons.
- **Electron Beam Focusing:** The electron beam is accelerated and focused using electromagnetic lenses. The focused electron beam forms a fine probe that can be scanned across the sample surface.
- **Sample Preparation:** Before imaging in the SEM, the sample must undergo appropriate preparation. It needs to be dehydrated, dried, and coated with a thin layer of conductive material (e.g., gold or carbon) to prevent charging effects during imaging.
- **Sample Interaction:** When the focused electron beam strikes the sample surface, several interactions occur between the electrons and the atoms in the sample. These interactions are responsible for generating various signals that are used to create the SEM image.
- **Secondary Electron Emission:** One of the primary interactions is the emission of secondary electrons from the sample's surface due to the impact of the incident electrons. These secondary electrons carry information about the surface topography and are used to create the SEM image.
- **Backscattered Electrons:** Some of the incident electrons experience elastic scattering, and they are backscattered from the sample's atomic nuclei. The energy of backscattered electrons is related to the average atomic number of the sample material, providing compositional contrast in the SEM image.

- **X-ray Emission:** Inelastic scattering of electrons can lead to the emission of characteristic X-rays from the sample. The energy and intensity of these X-rays can be used for elemental analysis (EDS or Energy Dispersive X-ray Spectroscopy) to determine the chemical composition of the sample.
- **Scanning and Image Formation:** The focused electron beam is scanned across the sample surface in a raster pattern. As the beam scans, signals from secondary electrons, backscattered electrons, and X-rays are detected and processed to form the SEM image. The brightness and contrast in the SEM image correspond to variations in the sample's surface properties, such as roughness, composition, and topography.
- **3D Imaging:** Advanced SEM systems can also use specialized techniques like electron beam lithography or focused ion beam (FIB) milling to create cross-sectional or 3D images of the sample, providing additional insights into the material's internal structure.

In summary, SEM works by scanning a focused electron beam across the sample's surface and detecting various signals generated from electron-sample interactions to create high-resolution images with detailed information about the sample's surface morphology, composition, and structure. SEM is widely used in materials science, nanotechnology, biology, geology, and many other fields for its ability to provide valuable insights into micro- and nano-scale structures.

The SEM is commonly equipped with an EDX device, which allows the chemical composition of the sample to be determined. EDX is an analytical method for examining X-rays emitted by a sample. When a high-energy electron beam strikes a sample, it may energize an electron in an inner shell, ejecting it from the level and creating an electron-

hole. A higher energy electron from an outer shell fills the electron hole, which is a place where the energy difference between the higher and lower energy levels can be discharged as an X-ray. An energy dispersive spectrometer can detect the energy emitted by a sample. The elemental composition of the specimen may be identified because the energy of the X-rays is proportional to the energy difference between the two levels and the atomic structure of the element from which they were emitted.

4.5 TEM (Transmission Electron Microscopy)

Transmission Electron Microscopy (TEM) is a powerful microscopy technique used to visualize and study the internal structure of materials at very high magnifications and resolution. Unlike Scanning Electron Microscopy (SEM) that images the surface of samples, TEM allows researchers to see through thin specimens and observe the arrangement of atoms and nanoscale structures within the sample. With this method, features are imaged by concentrating an electron beam on a spot that was transmitted through the specimens. A static electron beam interacts in TEM at accelerating voltages between 100 kV and 400 kV. The diffraction pattern is obtained from objective lenses through recombination of electrons. Due to the interaction of the electron with the sample, a device called photographic film is utilized to focus as well as magnify the image formed. The high-resolution image is obtained from TEM as compared to microscope and scanning electron microscopes.

4.5.1 Applications of TEM

TEM has several applications including:

- Conventional TEM (Morphology analysis at a nanoscale and phase and defect analysis)
- In-situ TEM (Structural change analysis)
- Analytical TEM (Chemical compositional analysis, Z-contrast imaging, and selected area electron diffraction pattern analysis)
- HRTEM (Lattice imaging, structural analysis of complex materials, interplanar d-spacing determination and atomic structure of defects)

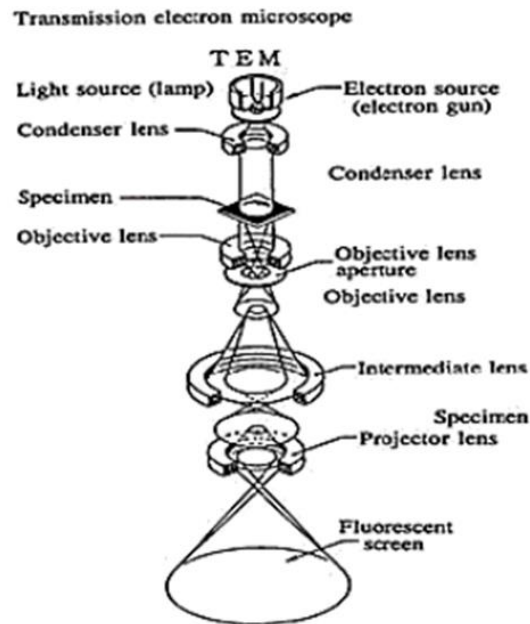


Figure 16: Illustration of TEM

4.6 XPS (X-Ray Photoelectron Spectroscopy)

X-ray Photoelectron Spectroscopy (XPS) is a surface-sensitive analytical technique used to determine the elemental composition and chemical state of materials. XPS works on the principle of photoelectric effect and the energy measurement of photoelectrons emitted from the surface of a sample when it is exposed to X-rays. X-ray photons with energies between 200 and 2000 eV are employed in XPS to detect the emission of photoelectrons from material surfaces. The energy of the excited photoelectrons aids in figuring out the compound's elemental composition.

4.6.1 Basic Principle and Mechanism

As a result of its surface impressionability, the photoelectrons generated close to the surface escape. The fundamental idea behind X-ray photoelectron spectroscopy (XPS) is that when a surface is bombarded with X-rays, electrons are ejected from it, producing photoelectrons. This method essentially relies on the photoelectric effect.

- **X-ray Source:** XPS uses a monochromatic X-ray source, typically an Al K α X-ray source, to generate X-rays with a specific energy. The X-ray energy is carefully chosen based on the properties of the material being studied.
- **Photoelectric Effect:** When X-rays with sufficient energy strike the surface of the sample, they interact with the electrons in the innermost atomic shells (core levels) of the atoms in the sample. The X-rays can cause the electrons in these core levels to be ejected from the atom. This process is known as the photoelectric effect.

- **Emission of Photoelectrons:** As a result of the photoelectric effect, core-level electrons are emitted from the sample and form a photoelectron signal.
- **Kinetic Energy Measurement:** The emitted photoelectrons have a kinetic energy that is characteristic of the element from which they originated and their specific chemical state. The kinetic energy is directly related to the energy of the X-rays used and the binding energy (binding energy is the energy required to remove the electron from the atom) of the core-level electron.
- **Energy Analyzer:** The emitted photoelectrons are then directed towards an energy analyzer, such as a hemispherical electron energy analyzer or a cylindrical mirror analyzer. This analyzer separates the photoelectrons based on their kinetic energy and measures their intensity as a function of kinetic energy.
- **Spectrum Acquisition:** By scanning the kinetic energy of the photoelectrons emitted from the sample, an XPS spectrum is obtained. The spectrum displays the number of photoelectrons detected at different kinetic energies, providing information about the core-level binding energies and chemical composition of the material.
- **Data Analysis:** The XPS spectrum is analyzed to identify the elements present in the sample and to determine their chemical states. Each element has characteristic binding energies, and the fine structure of the peaks in the spectrum provides information about the chemical environment of the element.

X-ray Photoelectron Spectroscopy is widely used in materials science, surface chemistry, catalysis, nanotechnology, and various other fields to analyze the surface composition and chemical bonding of solid materials. It provides valuable information about the elemental composition, oxidation states, and surface chemistry of materials,

making it a powerful tool for materials characterization and surface analysis.

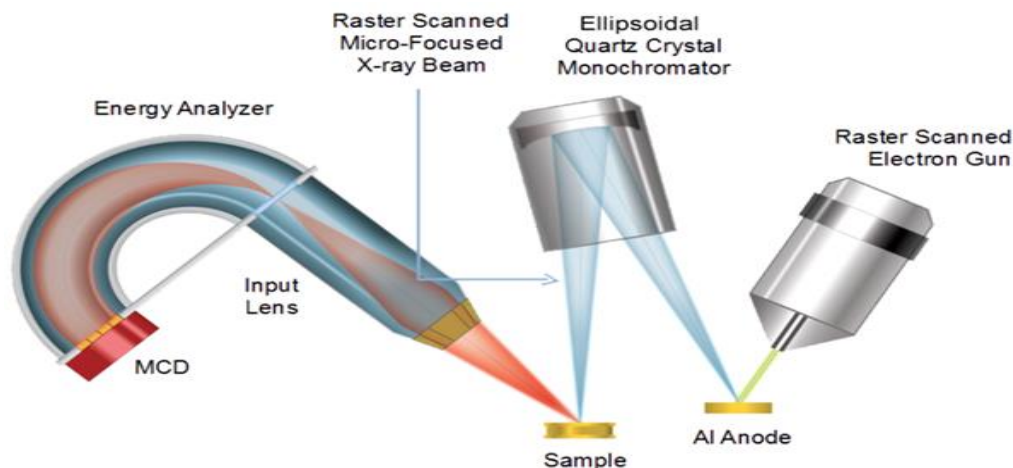


Figure 17: Illustration of XPS

4.7 Fourier Transform Infra-Red (FT-IR) Spectroscopy

FTIR spectrophotometric analysis involves the interaction of infrared radiation with matter. The energy of infrared radiation is low therefore when they interact with matter only vibrational and rotational movement is observed. The infrared region present in electromagnetic spectrum is separated into three portions i.e.,

- Near Infrared region
- Far infrared region
- Mid infrared region

Infrared spectroscopy is also called functional group spectroscopy. It is used for the functional group analysis of a chemical compound and from mode of transition and absorption value one can identify the chemical nature of given compound in the sample. Those chemical substances are identified in FTIR analysis in which a change in dipole moment occurs when infrared radiation falls on them. The change in dipole moment is necessary. In diametric symmetric molecules no dipole moment change is observed

therefore they do not show any vibrational motion in infrared regions, for example nitrogen. Asymmetric diatomic molecules like CO give IR spectrum due to change in its dipole moment as a result of interaction with infrared radiation. Complex molecules like organic molecules have many bonds thus can vibrate in different ways. There are basically two types of vibrations phenomena observed in FTIR spectroscopy i.e.,

- Stretching vibrations
- Bending Vibrations

4.7.1 Working Principle

The infrared spectrum of a sample is formed when infrared light passes through the sample. If the frequency of infrared radiation matches the frequency of chemical bond present in the analyte, then molecules show vibrational or rotational motion. The amount of light absorbed by analyte is measured. This gives information about the nature of chemical bonds and possible functional groups present in the sample. The source's IR beam enters the interferometer during the measurement and is directed towards a beam splitter. The beam is then split in half and pointed at a mirror that is both stationary and moving. The beam is then recombined and pointed towards the sample after that. In the meanwhile, complete wavelength spectrum data is acquired. The rotating mirror and light interference from the two split beams alter the optical path lengths. Since the optical pathways of both split beams are identical when the moving mirror's distance from the beam splitter is equal to that of the stationary mirror, there is no path difference. The beam-splitter is separated from the moving mirror by an optical path difference. Two split beams will frequently create both constructive and destructive interference, with a fluctuating value. The fast Fourier transform (FFT) method is used by a computer to produce the infrared spectrum.

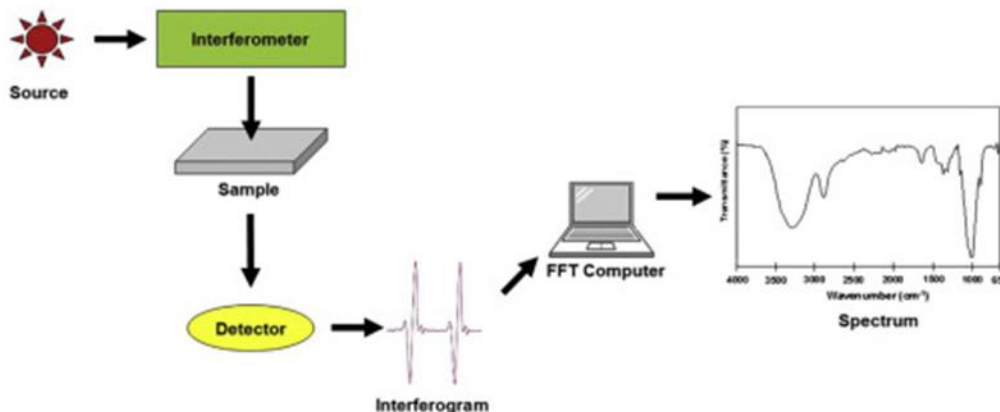


Figure 18: Illustration of instrumentation of FTIR

A chemical fingerprint may be compared to the FTIR spectrum. It may be used to characterize novel materials as well as recognize and validate known and unidentified samples. especially helpful in the industrial, chemical, and research & development sectors. FTIR spectroscopy may provide answers to a wide range of analytical issues in a number of sectors, depending on the spectrometer setup and process.

4.8 Brunauer, Emmett and Teller Analysis (BET)

The Brunauer-Emmett-Teller (BET) analysis is a widely used method for determining the specific surface area of porous materials, such as powders, catalysts, and adsorbents. It was developed by Stephen Brunauer, Paul Emmett, and Edward Teller in the late 1930s. The specific surface area is a crucial parameter in various fields, including materials science, chemistry, and engineering, as it affects the adsorption and reaction capabilities of these materials.

The BET analysis is based on the principle that gases, typically nitrogen, can be adsorbed onto the surface of a solid material due to the presence of pores and crevices. By measuring the amount of gas adsorbed at various pressures, the surface area of the material can be

determined. The BET method assumes that a single layer of gas molecules forms on the material's surface and that adsorption occurs in a multilayer manner.

4.8.1 Working Principle

The working principle of BET analysis involves several key steps:

- **Degassing:** The sample material is first degassed at elevated temperatures to remove any adsorbed impurities or gases that might interfere with the analysis. This ensures that the gas adsorption measured is due to the material's own surface.
- **Adsorption Isotherms:** The sample is exposed to a gas, typically nitrogen, at a range of increasing pressures. The amount of gas absorbed is recorded at each pressure point. The relationship between the amount of gas adsorbed and the pressure is called an adsorption isotherm.
- **Langmuir Monolayer:** At low pressures, gas molecules begin to adsorb onto the material's surface, forming a monolayer. The Langmuir adsorption model assumes that each adsorption site can accommodate only one gas molecule. However, this model is limited to low pressures and doesn't accurately represent adsorption behavior at higher pressures.
- **Multilayer Adsorption:** As pressure increases, additional gas molecules begin to adsorb onto the surface, forming multilayers. The BET theory assumes that these multilayers are physically indistinguishable, and the relative pressure at which multilayer adsorption begins is termed the "BET C value."
- **BET Equation:** The BET equation is used to correlate the amount of adsorbed gas with the relative pressure. It is given by:

$$\frac{V_m}{V} = \frac{C \cdot P}{(P_0 - P) \cdot (1 + C \cdot P)}$$

Where:

V_m is the volume of gas adsorbed at monolayer coverage.

V is the volume of gas adsorbed at the given pressure

C is the BET constant related to the energy of adsorption

P is the relative pressure

P_0 is the saturation pressure.

- **Surface Area Calculation:** The specific surface area of the material can be calculated from the slope of the BET plot, which is obtained by plotting $\frac{V_m}{V(P_0 - P)}$ against P . The slope of the linear portion of the plot gives the BET constant C , and from this constant, the specific surface area can be calculated using the Avogadro number and the cross-sectional area occupied by a nitrogen molecule.

The BET analysis provides valuable information about the porosity and surface characteristics of materials, making it an essential tool in various scientific and industrial applications.

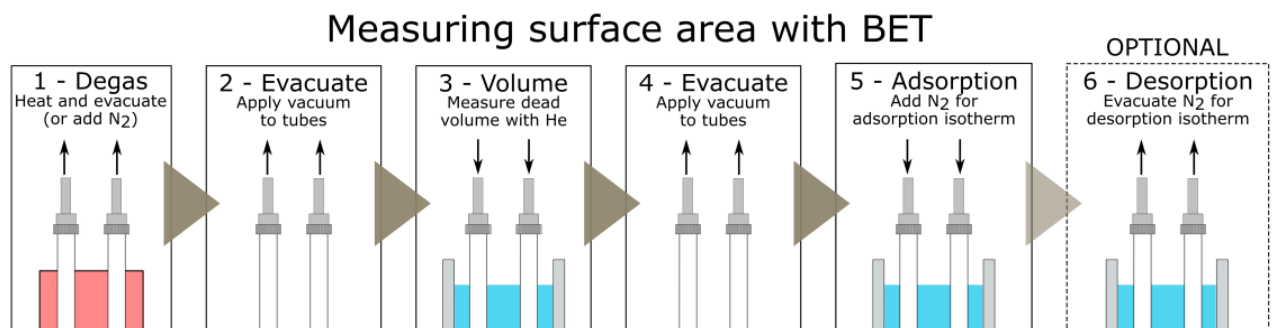


Figure 19: Illustration of working of BET analysis

4.9 Electrochemical Characterization

Electrochemical characterization for supercapacitors involves a series of tests and measurements to understand the device's performance, energy storage capacity, and efficiency. Supercapacitors, also known as ultracapacitors or electrochemical capacitors, are energy storage devices that bridge the gap between traditional capacitors and batteries. They store energy through reversible electrochemical processes at the electrode-electrolyte interfaces. Electrochemical characterization provides insights into their charge/discharge behavior, energy density, power density, cycle life, and other performance metrics. Generally speaking, this type of characterization refers to an in-situ method for tracking electrochemical redox processes and related follow-up reactions. We used a number of techniques, such as Cyclic voltammetry (CV), Electrochemical Impedance Spectroscopy (EIS), and Galvanostatic Charge/Discharge Analysis (GCD), to monitor the electrochemical performance of the electrodes which can be used in supercapacitors.

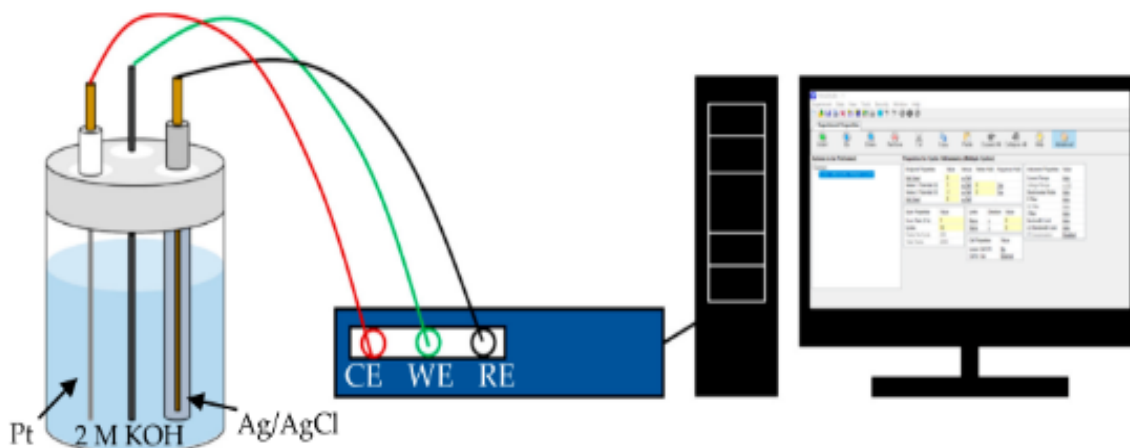


Figure 20: Illustration of three electrode system for various electrochemical characterization

4.9.1 Cyclic voltammetry (CV)

Cyclic Voltammetry (CV) is an electrochemical technique used to study the redox behavior and capacitive properties of materials in a three-electrode system. It's a fundamental

method employed for characterizing supercapacitors and other electrochemical devices. The three-electrode system consists of a working electrode, a reference electrode, and a counter electrode. In the context of supercapacitor characterization, the working electrode typically represents the supercapacitor electrode material, the reference electrode maintains a constant potential, and the counter electrode provides the current flow.

4.9.2. Working Principle

- **Setup:** In a three-electrode system for supercapacitors, the working electrode is immersed in an electrolyte solution, and it's connected to the external circuit. The reference electrode and counter electrode are also submerged in the electrolyte. The reference electrode maintains a stable potential against which the potential of the working electrode is measured. The counter electrode allows the passage of current between the working electrode and the reference electrode.
- **Potential Cycling:** In CV, the potential of the working electrode is cycled linearly between two preset values, typically from a more negative potential to a more positive potential and then back again. This potential range is called the "**potential window.**" As the potential changes, electrochemical reactions occur at the electrode-electrolyte interface.
- **Electrochemical Reactions:** During the forward scan (from negative to positive potential), the potential applied to the working electrode becomes more positive. Depending on the material of the working electrode, various electrochemical processes can occur, such as redox reactions, ion adsorption/desorption, or double-layer capacitance formation. These processes involve the movement of electrons and ions at the electrode-electrolyte interface.
- **Current Measurement:** As electrochemical reactions occur, a current flow between the working electrode and the auxiliary electrode. This current is measured and recorded at various potentials as the potential is swept within the specified range. The resulting current-potential curve is called a "voltammogram."

- **Reverse Scan:** After completing the forward scan, the potential is reversed and cycled back to the starting potential in the negative direction. This allows for the observation of reverse electrochemical reactions, and the corresponding current is recorded.

4.9.3 Interpretation

The cyclic voltammogram obtained from the CV experiment provides valuable information about the electrochemical behavior of the supercapacitor electrode material. The peaks and features in the voltammogram are related to specific electrochemical processes:

- **Anodic Peak:** An increase in current during the forward scan indicates an anodic reaction, which might involve oxidation or ion desorption from the electrode surface.
- **Cathodic Peak:** A decrease in current during the forward scan indicates a cathodic reaction, which could involve reduction or ion adsorption onto the electrode surface.
- **Double-Layer Capacitance:** The region near the reversible potential is associated with the formation of an electric double layer (EDL) at the electrode-electrolyte interface. The slope of this region provides information about the specific capacitance of the material.
- **Faradaic Processes:** Peaks away from the reversible potential can indicate faradaic reactions involving redox chemistry.

By analyzing the shape, position, and magnitude of peaks in the cyclic voltammogram, researchers can deduce important electrochemical parameters such as specific capacitance, reversibility of reactions, and overall performance of supercapacitor electrode materials.

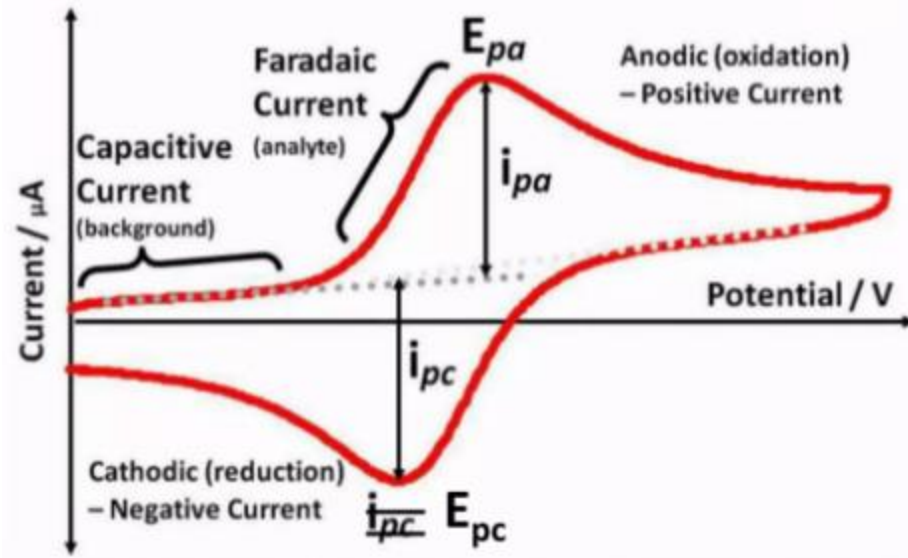


Figure 21: Cyclic voltammogram for an electrochemically reversible redox process

4.10 Galvanostatic Charge/Discharge Analysis (GCD)

Galvanostatic charge-discharge (GCD) is a form of electrochemical research that investigates the energy storage and discharge behavior of supercapacitors in a three-electrode setup. It provides insights into the capacitance, energy density, power density, and internal resistance of the supercapacitor electrode material. The three-electrode system consists of a working electrode, a reference electrode, and a counter electrode.

4.10.1 Working Principle

- **Initial State:** At the beginning of the experiment, the working electrode is in its initial state, which can be either fully charged or at an equilibrium potential.
- **Galvanostatic Charging:** In the galvanostatic charging phase, a constant current is applied to the working electrode. This current leads to the accumulation of charge on the electrode's surface, resulting in the charging of the electric double layer (EDL)

formed at the electrode-electrolyte interface. As charge accumulates, the voltage across the working electrode increases.

- **Monitoring Voltage:** During galvanostatic charging, the voltage across the working electrode is monitored over time. This voltage increases as more charge is stored on the electrode surface. The rate of voltage increase is influenced by the specific capacitance of the electrode material and the electrolyte's resistance.
- **Galvanostatic Discharging:** Once the desired charge level is reached or a specific charging time is completed, the constant current is switched off. The supercapacitor is then discharged at a constant current (the same magnitude as the charging current) in the galvanostatic discharging phase. As the discharge progresses, the voltage across the working electrode decreases.
- **Monitoring Voltage Drop:** During galvanostatic discharging, the voltage across the working electrode is monitored over time. The voltage drop occurs as the stored charge is released from the electrode surface. The rate of voltage drop is also affected by the electrode material's specific capacitance and the internal resistance of the supercapacitor.

4.10.2 Interpretation

The galvanostatic charge-discharge experiment provides important information about the supercapacitor's energy storage and discharge characteristics.

- **Charge and Discharge Curves:** The voltage-time curves obtained during the charge and discharge phases represent the supercapacitor's energy storage and release behavior. The slope of these curves indicates the capacitance of the device.
- **Voltage Drop:** The voltage drop during discharge gives insights into the internal resistance of the supercapacitor. A larger voltage drop indicates higher internal resistance, which affects the supercapacitor's overall performance.
- **Energy and Power Density:** The area under the discharge curve represents the energy stored by the supercapacitor. The ratio of the energy stored to the discharge time gives the power density.

By analyzing the charge and discharge curves, researchers can quantify the energy and power performance of supercapacitor electrode materials and evaluate their suitability for various applications.

4.11 Electrochemical Impedance Spectroscopy (EIS)

Electrochemical Impedance Spectroscopy (EIS) is a powerful technique used to analyze the electrochemical properties of supercapacitors and other electrochemical systems in a three-electrode setup. This method is widely employed for material impedance analysis. It is a sensitive approach that provides information on the composition of the material, the reaction mechanism, intermediates, and interface electrochemical reaction. Studies on sensing, corrosion, fuel, capacitors, and resistance make use of it. EIS provides valuable information about the internal processes, charge transfer kinetics, and resistive behavior of supercapacitor electrode materials.

4.11.1 Working Principle

The EIS is done at various frequencies. The real axis and the semicircle make up the two sections of the EIS curve. The qualities of the material determine the shape of the curve created during EIS testing. The true axis should be vertical, and the semicircle should be smaller for excellent systems, according to optimum capacitive materials. Analysis of the

Nyquist plot is used to calculate the value of resistances. To execute the z-fitting and assess the system's impedance, the proper circuit is chosen. The EIS spectra reveal several characteristic features that provide insights into the supercapacitor's behavior:

- **Electrolyte Resistance (R_s):** At high frequencies, the impedance is dominated by the solution resistance, which includes the resistance of the electrolyte and the resistance of the current path in the solution.
- **Charge Transfer Resistance (R_{ct}):** At intermediate frequencies, a semicircular feature appears in the impedance plot. This semicircle is associated with the charge transfer resistance, representing the resistance of charge transfer reactions at the electrode-electrolyte interface.
- **Double-Layer Capacitance (C_{dl}):** The radius of the semicircle is inversely proportional to the double-layer capacitance, which represents the capacitance of the electric double layer formed at the electrode-electrolyte interface.
- **Warburg Element (W):** At low frequencies, a sloping line in the impedance plot indicates the Warburg element, which corresponds to diffusion-limited processes occurring at the electrode-electrolyte interface.

By analyzing the impedance spectra and fitting them to equivalent circuit models, researchers can extract quantitative information about the supercapacitor's electrochemical processes, such as specific capacitance, charge transfer resistance, diffusion coefficients, and more. EIS is particularly useful for understanding the impact

of electrode materials, electrolyte properties, and electrode structure on the performance of supercapacitors.

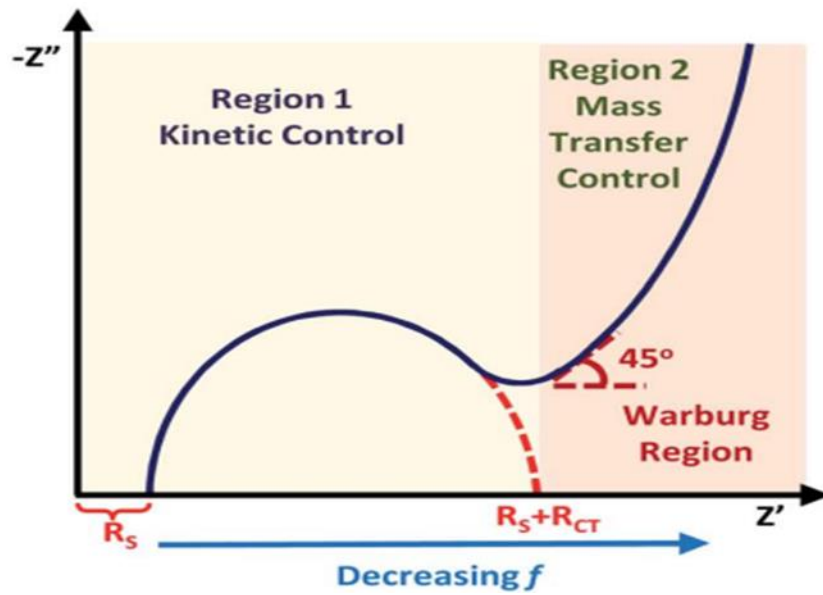


Figure 22: Nyquist plot with key regions labelled.

CHAPTER 5: RESULTS AND DISCUSSION

5.1 Morphological, Structural and Compositional analysis

5.1.1 X-Ray Diffraction Analysis (XRD)

The phase purity and crystal structure of the as prepared CC/NiCo₂O₄ and CC/NiCo₂O₄@SnS₂ samples were evaluated by XRD as shown in Figure 23. In CC/NiCo₂O₄ pattern, the major diffraction peaks located at 31.1°, 36.3°, 44.1° and 59.1° can be indexed to (220), (311), (400) and (511) planes correspond to the spinel cubic structure of NiCo₂O₄ (JCPDS card No:20-0781) [71]. Moreover, a wider diffraction peak at 26.3° can be observed due to the carbon cloth. The diffraction pattern of CC/NiCo₂O₄@SnS₂ shows diffraction peaks located at 14.7°, 28.4°, 31.4° and 50.1° corresponds to (001), (100), (101) and (110) planes of SnS₂ (JCPDS Card No: 23-0677) [72]. The presence of SnS₂ peaks confirms the successful formation of the nanostructures.

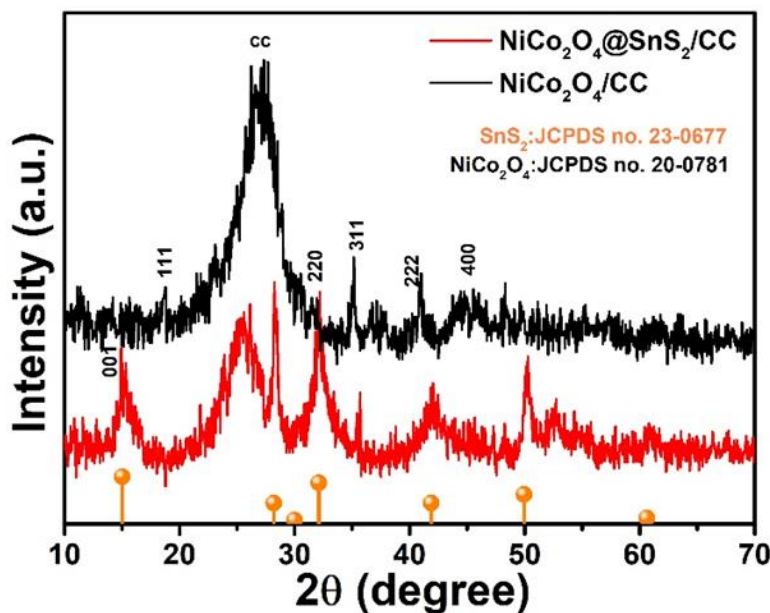


Figure 23: XRD Spectra of CC/NiCo₂O₄ and CC/NiCo₂O₄@SnS₂

5.1.2 Morphological Analysis

Figure 24 (a, b) shows the low and high magnification SEM images of pure carbon fibers which are straight with smooth surface. Figure 24 (c, d) displays the morphology of NiCo₂O₄ product grown on carbon cloth. It can be seen that each fiber is functionalized by a large number of nanosheets which are interconnected with one another in uniformly ordered arrays.

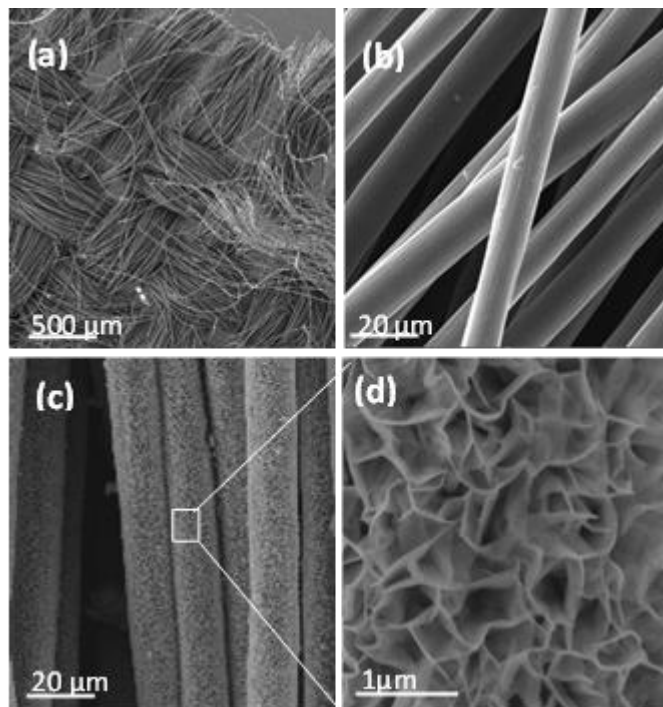


Figure 24: (a,b) Low and high magnification SEM image of carbon fibres (c,d) SEM image of NiCo₂O₄ nanostructures supported carbon fibres.

Figure 25 (a, b) displays the low and high magnification SEM images of CC/NiCo₂O₄@SnS₂ product and shows that SnS₂ hierarchical structure grow massively on CC/NiCo₂O₄ nanosheets. Such hierarchical networks of CC/NiCo₂O₄@SnS₂ nanosheets are highly useful because it makes easier for ions and electrons to diffuse through the material and penetrate during the electrochemical reactions. Figure (c) depicts the EDX spectrum of CC/NiCo₂O₄@SnS₂ structure which consists of Ni, Co, O, C, Sn and S peaks, confirms the formation of CC/NiCo₂O₄@SnS₂ nanosheets. Figure 25 (d, e) represent the low magnification TEM images of CC/NiCo₂O₄@SnS₂. It can be observed that the surface of nanosheets is decorated with several SnS₂ structures. Figure 25 (f, g) displays the HRTEM images of CC/NiCo₂O₄@SnS₂ and shows the polycrystalline nature.

The calculated lattice fringe spacing of 0.24 nm and 0.32 nm are corresponding to (311) and (100) planes of NiCo₂O₄ and hexagonal SnS₂ respectively.

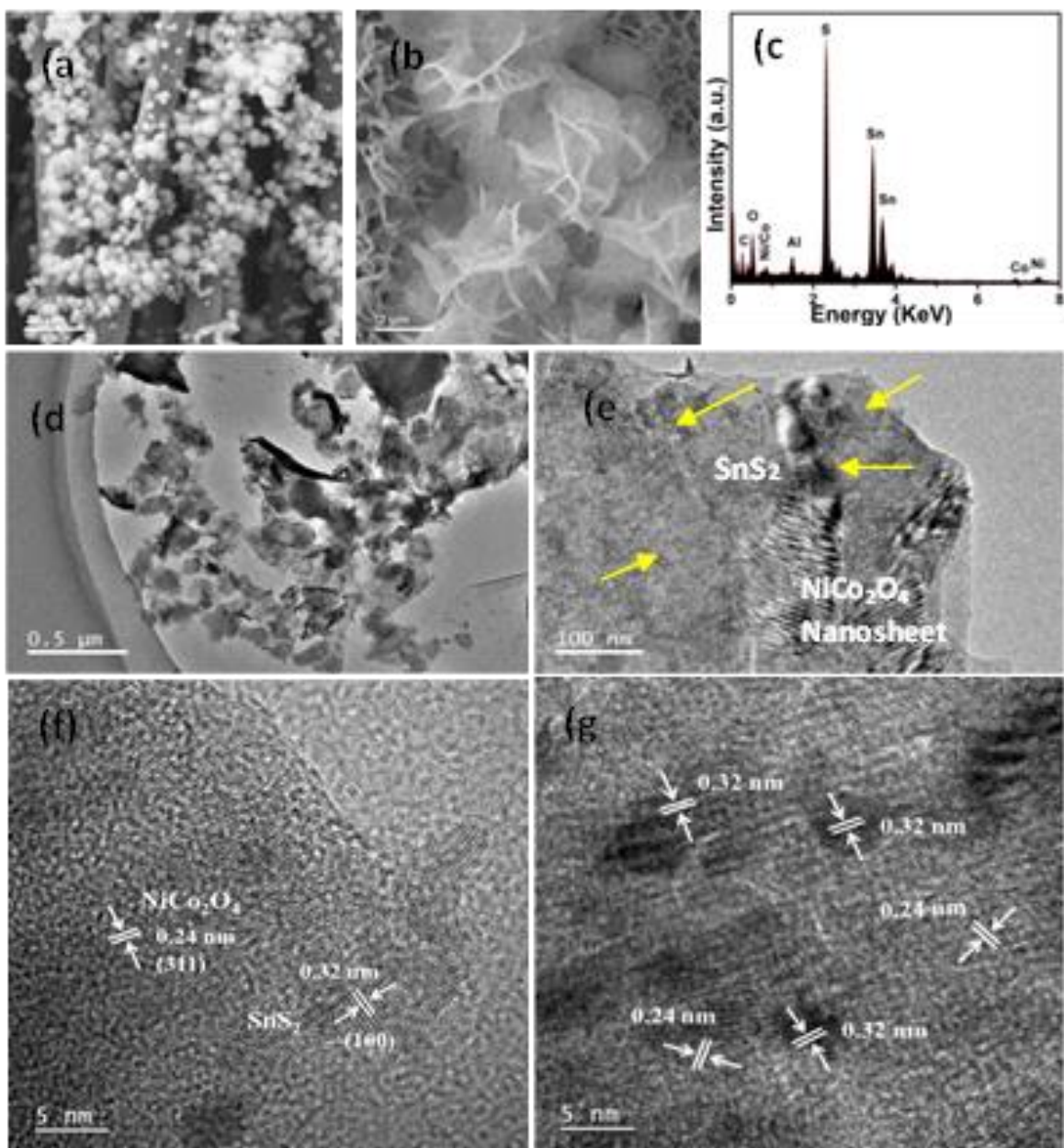


Figure 25: (a, b) low and high SEM images of CC/NiCo₂O₄@SnS₂ structures (c) corresponding EDX spectrum of CC/NiCo₂O₄@SnS₂ structure (d, e) Low and high magnification TEM images (f, g) High resolution TEM images of CC/NiCo₂O₄@SnS₂ structures

Moreover, Figure 26 (a-f) displays the STEM images of CC/NiCo₂O₄@SnS₂ structure and a corresponding elemental mapping of Ni, Co, Sn, S and O respectively. The presence of Sn and S confirms the deposition of SnS₂ and no other impurities formed other than NiCo₂O₄ and SnS₂ on carbon cloth.

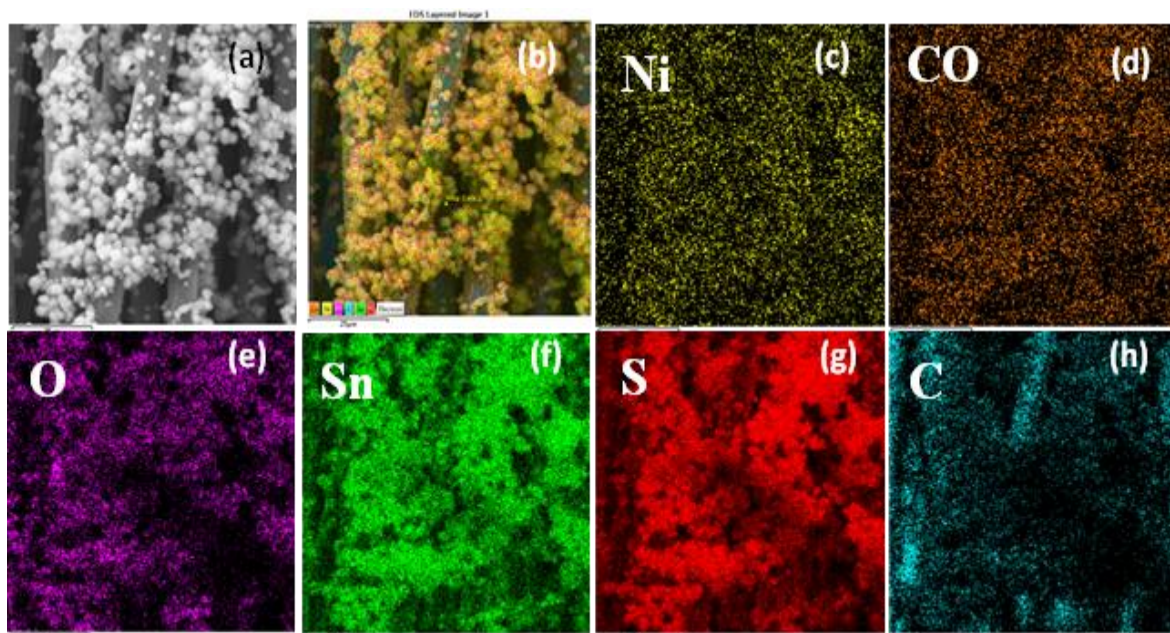


Figure 26: (a). STEM image of CC/NiCo₂O₄@SnS₂ nanostructures (b-h)EDS elemental mapping analysis for Ni, Co, O, C, Sn and S in CC/NiCo₂O₄@SnS₂ nanosheets

5.1.3 Fourier Transform Infra-Red Spectroscopy (FTIR)

Figure 27 displays the FTIR spectra of the as obtained CC/NiCo₂O₄ and the CC/NiCo₂O₄@SnS₂ nanostructures. The two typical NiCo₂O₄ absorption bands appear at 662 and 553cm⁻¹ which corresponds to the metal-oxygen stretching of Co-O and Ni-O vibrations from tetrahedral and octahedral sites, respectively. The O-H stretching and bending vibrations of the adsorbed water molecules are responsible for the broad bands at 3488cm⁻¹. Asymmetric stretching vibrations caused the detection of bands at 1606 and

1349 cm^{-1} [73]. Also the typical peaks of carbon cloth positioned at 2852 and 2923 cm^{-1} can be observed [74]. Additionally, the existence of the carboxylic group is represented by the peak at 1711 cm^{-1} . Some novel peaks located at 538 and 419 cm^{-1} are associated with the Sn-S bond which confirms the presence of SnS₂ in the CC/NiCo₂O₄@SnS₂ nanosheets [75].

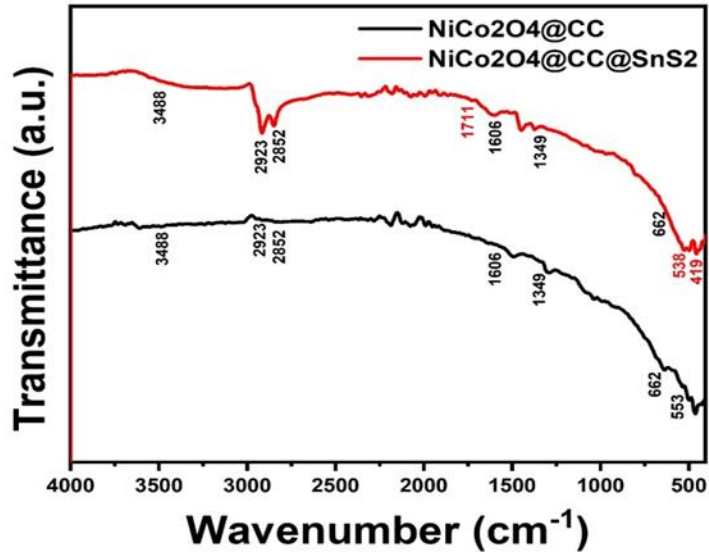


Figure 27: FTIR spectra of CC/NiCo₂O₄ and CC/NiCo₂O₄@SnS₂ structures

5.1.4 RAMAN Analysis

Figure 28 demonstrates the typical Raman spectra of CC@NiCo₂O₄ and CC@NiCo₂O₄@SnS₂ samples. In CC@NiCo₂O₄ spectrum, the peaks at 181.1 cm^{-1} , 461.5 cm^{-1} , 509.1 cm^{-1} , and 618.1 cm^{-1} are ascribed to the F_{2g}, E_g, L_o, and A_{1g} vibrational modes respectively [76]. Moreover, the peaks located at 1348.1 cm^{-1} and 1590.1 cm^{-1} are related to the D and G bands of compositional appearance of carbon cloth [77]. The ratio of D to G bands (I_D/I_G) ~1.3 indicates minor structural defects. Whereas, the CC@NiCo₂O₄@SnS₂ spectrum consists of a strong peak at 310 cm^{-1} and a broad band centered at 214 cm^{-1} demonstrates the existence of A_{1g} and E_g modes of SnS₂ [78].

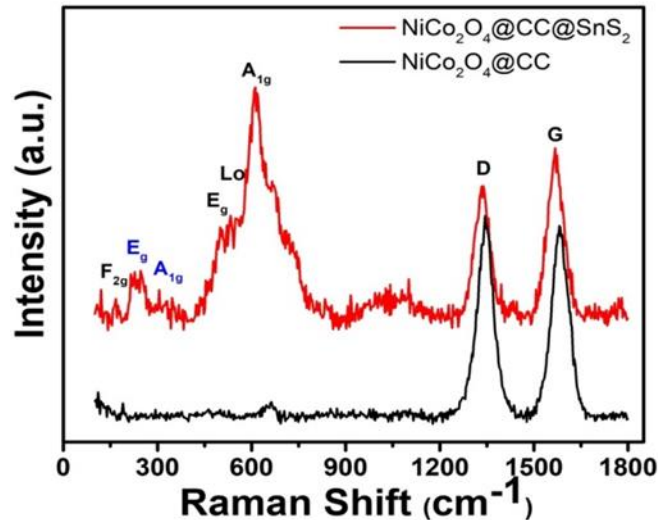


Figure 28: Raman spectra of CC/NiCo₂O₄ and CC/NiCo₂O₄@SnS₂ structures

5.1.5 X-ray Photoelectron Spectroscopy (XPS)

XPS was used to analyze the valence states of the surface atoms since they have a significant impact on the electrocatalytic efficiency of electrode material. Figure 29 (a) shows the deconvoluted XPS spectrum of C 1s which consists of three peaks located at 284.8eV, 286.1eV and 288.6 eV referred to the C-C, C-O-C, and O-C=O functional groups respectively [79]. Figure 29 (b) exhibits spectrum of Ni 2p that has two primary peaks. The coexistence peaks of Ni³⁺ and Ni²⁺ states are situated in the Ni 2p_{3/2} area at 855.4 and 857.1eV, respectively, whereas the Ni 2p_{1/2} region exhibits coexistence peaks at 873.2eV (Ni³⁺) and 875.4eV (Ni²⁺). Instead of significant peaks, there are two shake-up satellite peaks at 862.4 and 880.3eV, which are associated with Ni 2p_{3/2} and Ni 2p_{1/2}, respectively. It is already known that the presence of Ni³⁺ and Ni²⁺ states play significant role in the electrochemical performance of the electrode. Figure 29 (c) depicts the high-resolution

spectrum of Co 2p peak. It shows two major peaks located at 781.3 and 797.4eV, respectively, corresponding to the electronic states of Co 2p_{3/2} and Co 2p_{1/2} respectively. The fitting results demonstrate coexistence of Co³⁺ and Co²⁺ states. The spectrum also shows satellite peaks at the higher binding energy area at 786.9 and 803.6eV [80]. Figure 29 (d) represents the XPS spectrum of O 1s peak which confirms oxygen contributions. The peak at 531.3 and 532.5 eV are attributed to oxygen-containing groups and metal-oxygen bonds, respectively. The XPS spectrum of Sn3d demonstrates two primary peaks at 494.7eV and 486.7eV correspond to Sn 3d_{3/2} and Sn 3d_{5/2} states as shown in Figure 29 (e) and confirms the presence of Sn in the structure [81]. Furthermore, the high resolution XPS spectrum of S 2p peak is displayed in Figure 29 (f). Two spin-orbit peaks at 161.3eV and 162.1eV are seen in the spectrum, which correspond to the S 2p_{3/2} and S 2p_{1/2} states, respectively.

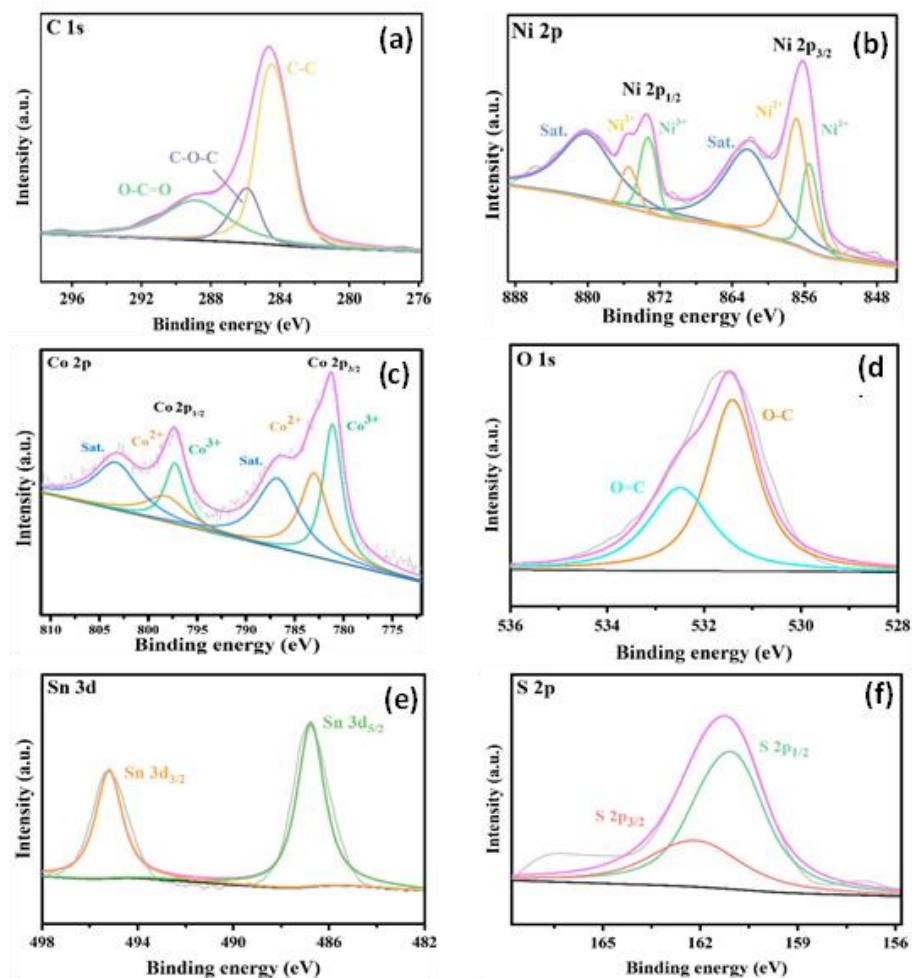


Figure 29: The high-resolution XPS spectra of CC/NiCo₂O₄ and CC/NiCo₂O₄@SnS₂ nanostructures (a) C 1s (b) Ni 2p (c) Co 2p (d) O 1s (e) Sn 3d and (f) S 2p

5.1.6 Brunauer, Emmett and Teller Analysis (BET)

The specific surface areas of the synthesized products are determined by measuring N₂ adsorption-desorption isotherms. Figure 30 displays the nitrogen adsorption-desorption isotherms for NiCo₂O₄ and NiCo₂O₄@SnS₂ at 77 K. In comparison to NiCo₂O₄ nanostructure, the isotherm of NiCo₂O₄@SnS₂ nanosheets exhibits a considerably broader hysteresis loop. For NiCo₂O₄@SnS₂ and NiCo₂O₄, the corresponding BET specific surface areas are (80.5 m²/g) and (51.5 m²/g), respectively. This demonstrates indisputably that the

NiCo₂O₄@SnS₂ nanosheets has a greater surface area than NiCo₂O₄ due to the interconnected NiCo₂O₄@SnS₂ nanostructures. The Specific surface area is a well-known feature that significantly affects the electrochemical properties of electrode materials. Therefore, the greater electroactive surface area of NiCo₂O₄@SnS₂ nanosheets contributes a significant role in electrochemical processes and is considered more suitable materials for biosensing and supercapacitor applications.

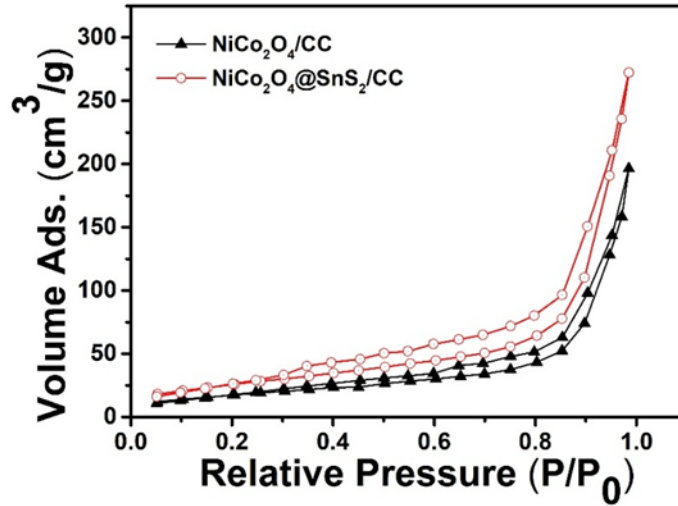


Figure 30: BET specific surface area of CC/NiCo₂O₄ and CC/NiCo₂O₄@SnS₂ structures

5.2 Electrochemical Characterization Techniques

5.2.1 Cyclic Voltammetry (CV)

The electrochemical capacitive behavior of CC/NiCo₂O₄ and CC/NiCo₂O₄@SnS₂ electrodes was investigated by CV measurements. Figure 31 shows the comparative CV curves of both electrodes at a scan rate of 5 mVs⁻¹ in a voltage window of -0.4 to 0.6V and depicts the pseudo capacitive behavior. As clearly observed, the CC/NiCo₂O₄@SnS₂ electrode reveals significant enhanced current response and the high areal specific capacitance compared to CC/NiCo₂O₄ electrode. Figure (b) and Figure (c) demonstrate the CV curves of CC/NiCo₂O₄ and CC/NiCo₂O₄@SnS₂ electrodes respectively, measured at

different scan rates ranging from 2 to 40 mVs^{-1} . The pair of peaks at higher potential is associated with the fast reversible faradaic redox reactions of transition-metal ions with the electrolyte. The CV curves of $\text{CC/NiCo}_2\text{O}_4@\text{SnS}_2$ electrode show that the redox reaction is influenced by the change in scan rates. It can be seen that the current response increases with the increase in scan rate. The shape of the CV curves remains similar even at high scan rate which shows that the $\text{CC/NiCo}_2\text{O}_4@\text{SnS}_2$ structure reveals great electrochemical reversibility and high-rate performance. The enhanced response of $\text{CC/NiCo}_2\text{O}_4@\text{SnS}_2$ electrode indicates that the addition of SnS has strong influenced due to increase in number of active sites.

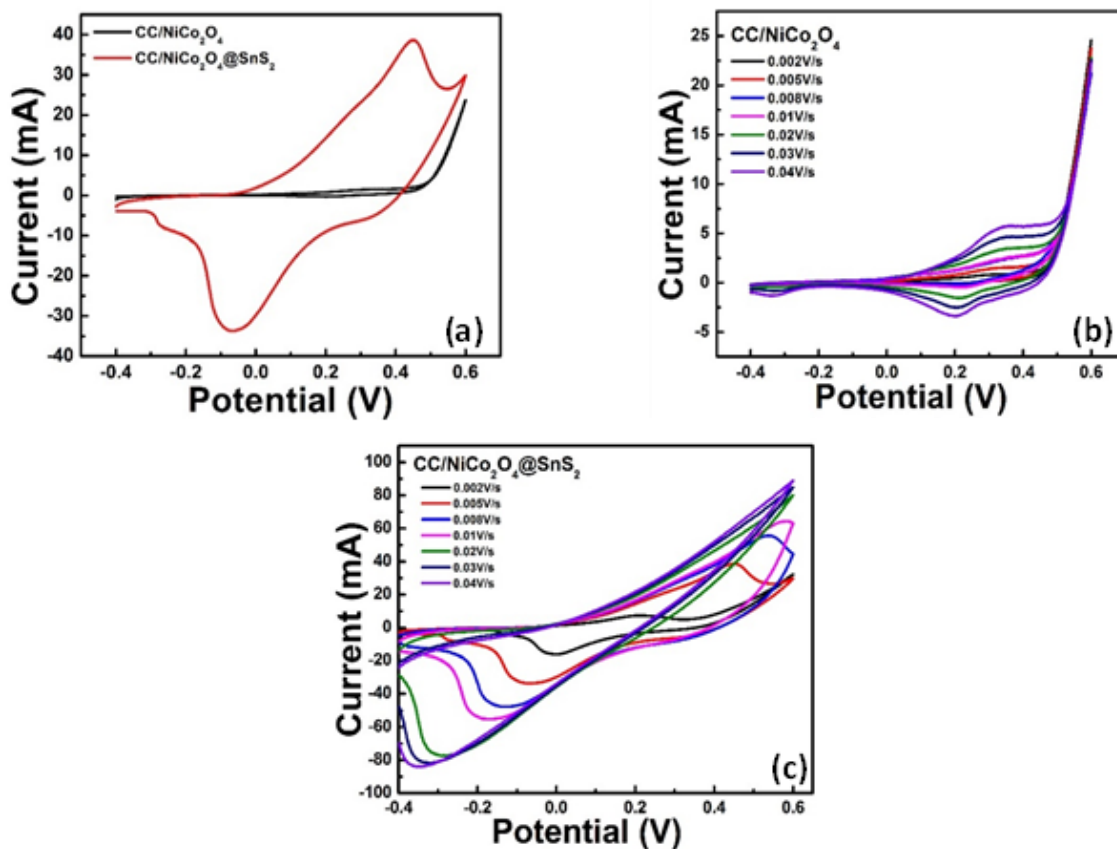


Figure 31: (a) Comparison of CV curves of CC/NiCo₂O₄ and CC/NiCo₂O₄@SnS₂ electrodes (b-c) CV curves of CC/NiCo₂O₄ and CC/NiCo₂O₄@SnS₂ structures at different scan rates

5.2.2 Galvanostatic Charge and Discharge (GCD)

The performance of both electrodes is evaluated by recording galvanostatic charge-discharge behavior. Figure 32 (a) shows the comparative curves of both electrodes at a current density of 2 A g^{-1} . It can be observed that CC/NiCo₂O₄@SnS₂ has longer discharge time as compared to CC/NiCo₂O₄ electrode. The triangular shape of the curves shows that both electrodes have good reversibility during the charge and discharge process. Figure 32 (b,c) shows the GCD curves of both electrodes at different current densities ranging from 2 to 10 A g^{-1} in a potential window of 0.0 to 0.5 V. The specific capacitance of CC/NiCo₂O₄@SnS₂ electrode at current densities of 2, 4, 6, 8, and 10 A g^{-1} is calculated

by GCD curves to be 655.7, 492, 451.8, 420.3 and 185 F/g respectively. For comparison, the GCD curves of CC/NiCo₂O₄ electrode at different current densities are also conducted as shown. The maximum specific capacitance is obtained at 2 A g⁻¹.

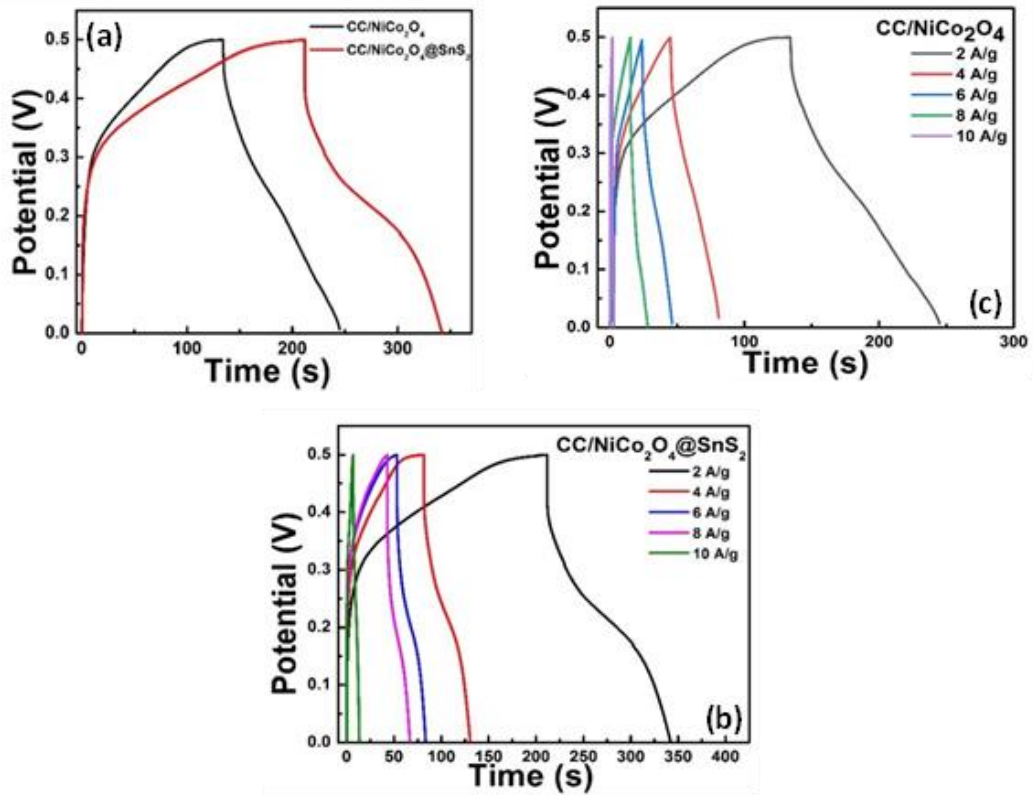


Figure 32: (a) Comparison of GCD curves of CC/NiCo₂O₄ and CC/NiCo₂O₄@SnS₂ electrodes (b-c) GCD curves of CC/NiCo₂O₄ and CC/NiCo₂O₄@SnS₂ structures at different current densities

5.2.3 Rate Performance

Figure 33 (a) shows the comparative plots of specific capacitance of both electrodes calculated at different current densities ranging from 2 to 10 A g⁻¹. It can be observed that the CC/NiCo₂O₄@SnS₂ electrode has an increased specific capacitance of 655.7 F/g at 2A g⁻¹ as compared to CC/NiCo₂O₄ (560 F/g) and proves that CC/NiCo₂O₄@SnS₂ electrode exhibits better rate performance. To determine the electrochemical performance of supercapacitors, the energy density (E, Wh/kg) and power density (P, W/kg) for Ragone plot are calculated by using the Eqs. (1) and (2) [82]. Figure 33 (b) displays the Ragone plot of CC/NiCo₂O₄ and CC/NiCo₂O₄@SnS₂ electrodes.

$$E = \frac{C_s V^2}{(3.6 \times 2)} (1)$$

$$P = \frac{3600E}{t} (2)$$

Where, E and P are energy density (Wh/kg) and power density (W/kg), C_s (F/g) is the specific capacitance in a three-electrode system, V (V) is the voltage window and t (s) is the discharge time. This plot depicts that the CC/NiCo₂O₄@SnS₂ electrode can provide an energy density of 14.7 Wh kg⁻¹ at a power density of 393 W kg⁻¹.

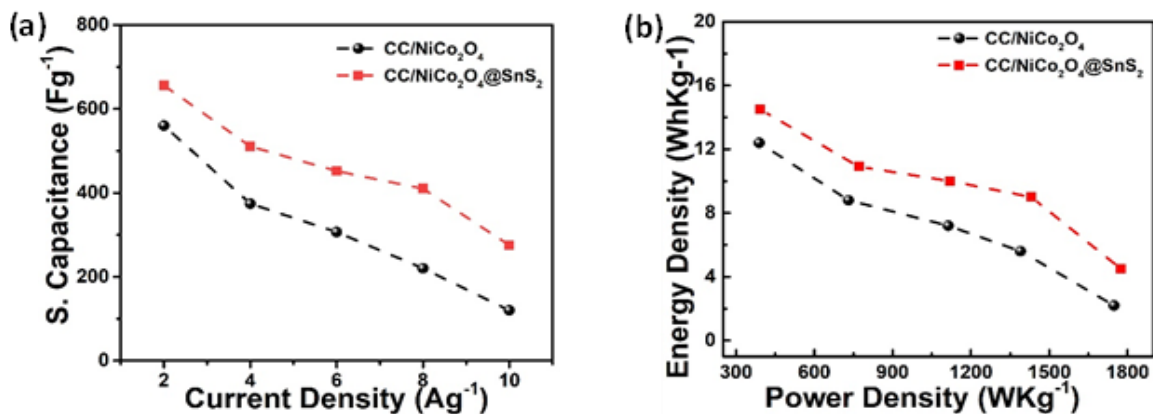


Figure 33: (a) Comparison of specific capacitance of CC/NiCo₂O₄ and CC/NiCo₂O₄@SnS₂ at different current densities of 2 to 10 Ag⁻¹ (b) Comparison of the Ragone plots of CC/NiCo₂O₄ and CC/NiCo₂O₄@SnS₂ electrodes

5.2.4 Cyclic Performance

The study of cyclic stability is also a key factor to determine the electrode lifespan. Figure 34 presents the cyclic stability graph of the CC/NiCo₂O₄ and CC/NiCo₂O₄@SnS₂ electrodes at a current density of 4 A/g for 10,000 charge-discharge cycles. It can be observed that the CC/NiCo₂O₄@SnS₂ electrode exhibits excellent stability than CC/NiCo₂O₄ electrode. Also, at constant current density of 4A g⁻¹, the electrode retained 95.3 % of its original capacitance after 10,000 cycles of operation, demonstrating excellent cycling performance as compare with previously reported electrodes (Table 4). The stable performance of the electrode is suggested due to the strong interaction between two materials, good structural features and an increased number of active sites. The cyclic performance results show that CC/NiCo₂O₄@SnS₂ structure is a suitable candidate for the fabrication of stable and high-performance supercapacitor.

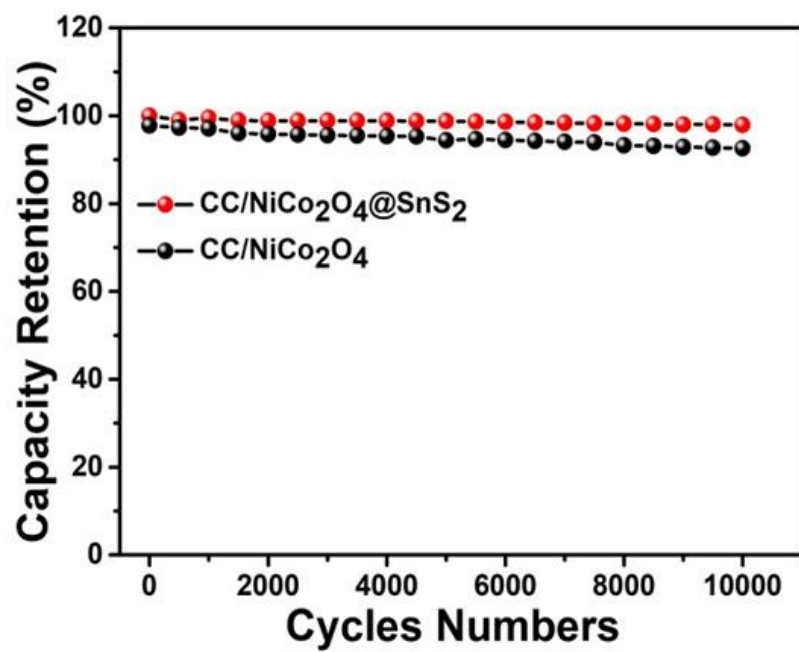


Figure 34: Cyclic performance of CC/NiCo₂O₄ and CC/NiCo₂O₄@SnS₂ at 2 Ag-1

Table 4: Comparative analysis of various electrochemical materials used as an electrode for high performance supercapacitors

No.	Material	Specific capacitance (F g ⁻¹)	Current density (A g ⁻¹)	Cycle Numbers	Cycling stability (%)	Ref
1.	NiCo ₂ O ₄ nanorods	233	1	2000	94	[83]
2.	NiCo ₂ S ₄ @NiFe LDH	827	1	12000	90.2	[84]
3.	ZnFe ₂ O ₄ /GO	352.9	1	10000	92.3	[85]
4.	Ni/Co-MOF nanoflakes	530.4	0.5	–	–	[86]
5.	SnS ₂ particles	93.8	0.5	500	95	[87]
6.	CF-SnS ₂	524.5	0.08	1000	68	[88]

7.	SnS ₂ nanosheets	89.4	1	1000	–	[89]
8.	NiS ₂ NPs@CNF	364.8	0.5	5000	92.8	[90]
9.	NiFe ₂ O ₄ @rGO	488	1	10000	89.8	[91]
10.	Mn doped SnO ₂ @MoS ₂	242	0.5	5000	83.9	[92]
11.	CoS ₂ -CNFs	488	1	–	91	[93]
12.	NiCo ₂ S ₄ /AC	150.9	1	–	–	[94]

13.	CuS ₄ @CC	485	0.25	1000	80.2	[95]
14.	Co-Ni-OH/rGO/CC	151.4	2.5	1000	88	[96]
15.	CC/NiCo₂O₄	560.0	2	10,000	92.5	This work
16.	CC/NiCo₂O₄@SnS₂	655.7	2	10,000	95.3	This work

5.2.5 Electrochemical Impedance Spectroscopy

EIS measurements are also conducted to further examine the reaction kinetics and charge transfer resistance. The relative Nyquist plots of the CC/NiCo₂O₄@SnS₂ and CC/NiCo₂O₄ electrodes in a 3 M KOH electrolyte are displayed in Figure 35. Due to the charge transfer resistance (R_{ct}) at the electrode/electrolyte interface, the semi-circle is formed in the high-frequency region and the corresponding series resistance is represented by the intercept in the x-axis (R_s). The diffusion-limited process is connected to the sloped straight line at low frequency. It is clear from the plots that the CC/NiCo₂O₄@SnS₂ electrode exhibits a smaller semi-circle and steeper slope. The experimental data is well fitted by the equivalent circuit model using Z-view software. The calculated kinetic parameters of CC/NiCo₂O₄@SnS₂ electrode are $R_s(0.55 \Omega)$ and $R_{ct}(38.4\Omega)$ which are smaller as compared to CC/NiCo₂O₄ electrode indicating superior kinetics in the electrochemical process. The enhanced kinetics of the CC/NiCo₂O₄@SnS₂ electrode are attributed to the formation of additional active sites, which effectively improve the electron transport characteristics. Because of its low charge transfer resistance and quick ion/electron transfer, the CC/NiCo₂O₄@SnS₂ electrode is considered an excellent choice for a long-lasting material for the development of supercapacitor.

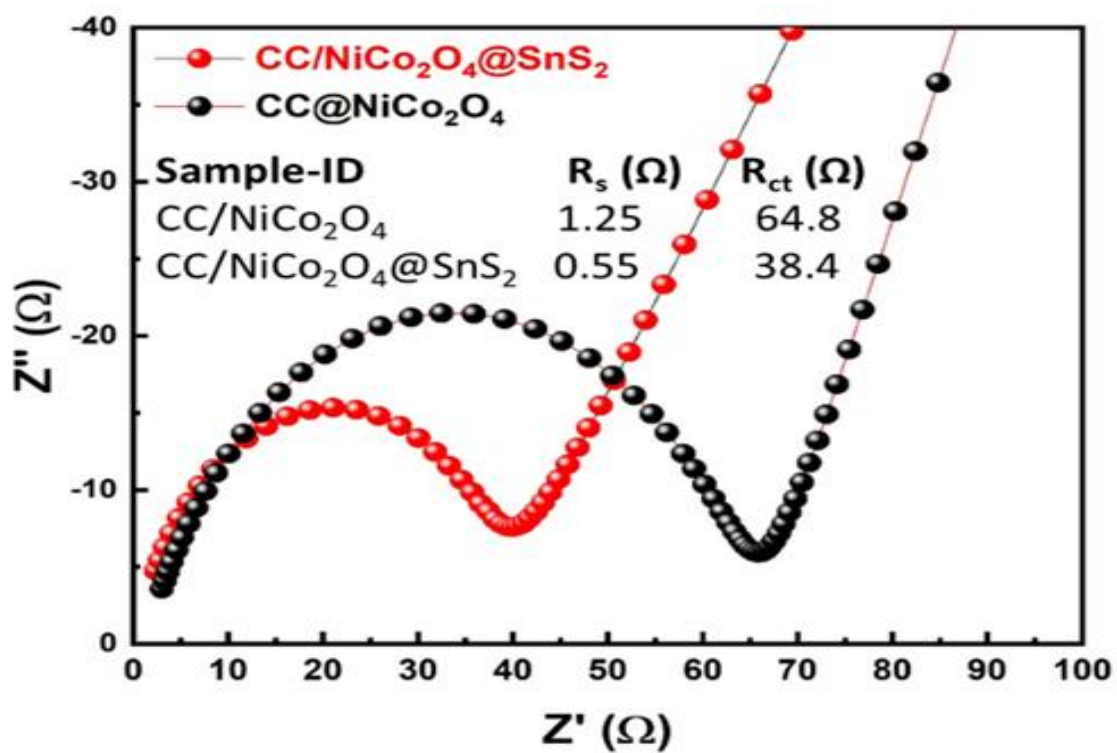


Figure 35: Comparison of the EIS curves of CC/NiCo₂O₄ and CC/NiCo₂O₄@SnS₂ electrodes; inset is the kinetic parameters of both electrodes.

CHAPTER 6: CONCLUSION AND FUTURE RECOMMENDATIONS

In summary, NiCo₂O₄@SnS₂ structure was successfully synthesized on CC by a facile hydrothermal process. The as-prepared nanostructures reveal that the NiCo₂O₄@SnS₂ nanostructure offers a large surface area for ion adsorption and enhances ion transport, leading to fabricate electrode for high performance supercapacitor. The developed electrode has an excellent specific capacitance of 655.7 F/g at 2Ag⁻¹. The electrode keeps 95.3 % of its preliminary capacitance after 10,000 cycles and providing an excellent cyclic stability. The significant improved performance of the electrode is associated to the rich active sites as well as synergistic effects of the multi-components. The results demonstrate that a NiCo₂O₄@SnS₂ composite provides a novel platform for the fabrication of supercapacitors.

REFERENCES

- [1] L. Huang, W. Zhang, J. Xiang, H. Xu, G. Li, and Y. Huang, "Hierarchical core-shell NiCo₂O₄@NiMoO₄ nanowires grown on carbon cloth as integrated electrode for high-performance supercapacitors," *Sci Rep*, vol. 6, 2016, doi: 10.1038/srep31465.
- [2] X. Han, X. Gui, T.-F. Yi, Y. Li, and C. Yue, "Recent progress of NiCo₂O₄-based anodes for high-performance lithium-ion batteries," *Curr Opin Solid State Mater Sci*, vol. 22, no. 4, pp. 109–126, 2018.
- [3] A. Riaz, M. R. Sarker, M. H. M. Saad, and R. Mohamed, "Review on comparison of different energy storage technologies used in micro-energy harvesting, WSNs, low-cost microelectronic devices: challenges and recommendations," *Sensors*, vol. 21, no. 15, p. 5041, 2021.
- [4] M. E. Sahin, F. Blaabjerg, and A. Sangwongwanich, "A review on supercapacitor materials and developments," *Turkish Journal of Materials*, vol. 5, no. 2, pp. 10–24, 2020.
- [5] U. S. Sani and I. H. Shanono, "A Review on Supercapacitors," *Akgec International Journal of Technology*, 2016.
- [6] J. Libich, J. Máca, J. Vondrák, O. Čech, and M. Sedlaříková, "Supercapacitors: Properties and applications," *J Energy Storage*, vol. 17, pp. 224–227, 2018.
- [7] H. Abedi, F. Migliorini, R. Dondè, S. De Iuliis, F. Passaretti, and C. Fanciulli, "Small size thermoelectric power supply for battery backup," *Energy*, vol. 188, p. 116061, 2019.
- [8] S. Sagaria, R. C. Neto, and P. Baptista, "Assessing the performance of vehicles powered by battery, fuel cell and ultra-capacitor: Application to light-duty vehicles and buses," *Energy Convers Manag*, vol. 229, p. 113767, 2021.

- [9] A. Shellikeri *et al.*, “Hybrid lithium-ion capacitor with LiFePO₄/AC composite cathode—long term cycle life study, rate effect and charge sharing analysis,” *J Power Sources*, vol. 392, pp. 285–295, 2018.
- [10] Y. Ma *et al.*, “A two step approach for making super capacitors from waste wood,” *J Clean Prod*, vol. 279, p. 123786, 2021.
- [11] B. E. Conway, *Electrochemical supercapacitors: scientific fundamentals and technological applications*. Springer Science & Business Media, 2013.
- [12] V. V Jadhav, R. S. Mane, and P. V Shinde, *Bismuth-Ferrite-Based Electrochemical Supercapacitors*. Springer, 2020.
- [13] R. Kötz and M. Carlen, “Principles and applications of electrochemical capacitors,” *Electrochim Acta*, vol. 45, no. 15–16, pp. 2483–2498, 2000.
- [14] K. Komatsubara *et al.*, “Highly oriented carbon nanotube supercapacitors,” *ACS Appl Nano Mater*, vol. 5, no. 1, pp. 1521–1532, 2022.
- [15] S. Banerjee, B. De, P. Sinha, J. Cherusseri, and K. K. Kar, “Applications of supercapacitors,” *Handbook of Nanocomposite Supercapacitor Materials I: Characteristics*, pp. 341–350, 2020.
- [16] A. Afif, S. M. H. Rahman, A. T. Azad, J. Zaini, M. A. Islan, and A. K. Azad, “Advanced materials and technologies for hybrid supercapacitors for energy storage—A review,” *J Energy Storage*, vol. 25, p. 100852, 2019.
- [17] J. Chen and P. S. Lee, “Electrochemical supercapacitors: from mechanism understanding to multifunctional applications,” *Adv Energy Mater*, vol. 11, no. 6, p. 2003311, 2021.
- [18] A. Vlad, N. Singh, J. Rolland, S. Melinte, P. M. Ajayan, and J.-F. Gohy, “Hybrid supercapacitor-battery materials for fast electrochemical charge storage,” *Sci Rep*, vol. 4, no. 1, p. 4315, 2014.

- [19] L. Xu, L. Zhang, B. Cheng, and J. Yu, "Rationally designed hierarchical NiCo₂O₄-C@Ni(OH)₂ core-shell nanofibers for high performance supercapacitors," *Carbon N Y*, vol. 152, pp. 652–660, 2019.
- [20] J. Du *et al.*, "Ultrathin porous NiCo₂O₄ nanosheet arrays on flexible carbon fabric for high-performance supercapacitors," *ACS Appl Mater Interfaces*, vol. 5, no. 15, pp. 7405–7409, 2013.
- [21] B. Saravanakumar, T. Priyadharshini, G. Ravi, V. Ganesh, A. Sakunthala, and R. Yuvakkumar, "Hydrothermal synthesis of spherical NiCO₂O₄ nanoparticles as a positive electrode for pseudocapacitor applications," *J Solgel Sci Technol*, vol. 84, pp. 297–305, 2017.
- [22] H. Xia, J. Zhang, Z. Yang, S. Guo, S. Guo, and Q. Xu, "2D MOF nanoflake-assembled spherical microstructures for enhanced supercapacitor and electrocatalysis performances," *Nanomicro Lett*, vol. 9, pp. 1–11, 2017.
- [23] B. Saravanakumar, T. Priyadharshini, G. Ravi, V. Ganesh, A. Sakunthala, and R. Yuvakkumar, "Hydrothermal synthesis of spherical NiCO₂O₄ nanoparticles as a positive electrode for pseudocapacitor applications," *J Solgel Sci Technol*, vol. 84, pp. 297–305, 2017.
- [24] H. Chauhan, M. K. Singh, P. Kumar, S. A. Hashmi, and S. Deka, "Development of SnS₂/RGO nanosheet composite for cost-effective aqueous hybrid supercapacitors," *Nanotechnology*, vol. 28, no. 2, p. 025401, 2016.
- [25] N. M. Soudagar, V. K. Pandit, R. B. Pujari, K. B. Chorghade, C. D. Lokhande, and S. S. Joshi, "Chemically synthesized polyaniline supercapacitor," *J. Eng. Res. Technol*, vol. 1, no. 10, 2017.
- [26] S. S. Rabbani *et al.*, "Nickel foam supported hierarchical NiCo₂S₄@NiFe LDH heterostructures as highly efficient electrode for long cycling stability supercapacitor," *Electrochim Acta*, vol. 446, p. 142098, 2023.

- [27] H. Chauhan, M. K. Singh, P. Kumar, S. A. Hashmi, and S. Deka, "Development of SnS₂/RGO nanosheet composite for cost-effective aqueous hybrid supercapacitors," *Nanotechnology*, vol. 28, no. 2, p. 025401, 2016.
- [28] V. V Jadhav, R. S. Mane, P. V Shinde, V. V Jadhav, R. S. Mane, and P. V Shinde, "Electrochemical supercapacitors: history, types, designing processes, operation mechanisms, and advantages and disadvantages," *Bismuth-Ferrite-Based Electrochemical Supercapacitors*, pp. 11–36, 2020.
- [29] R. Ding, L. Qi, M. Jia, and H. Wang, "Facile and large-scale chemical synthesis of highly porous secondary submicron/micron-sized NiCo₂O₄ materials for high-performance aqueous hybrid AC-NiCo₂O₄ electrochemical capacitors," *Electrochim Acta*, vol. 107, pp. 494–502, 2013.
- [30] A. Manalu *et al.*, "Synthesis, Microstructure and Electrical Properties of NiCo₂O₄/rGO Composites as Pseudocapacitive Electrode for Supercapacitors," *Int J Electrochem Sci*, vol. 22036, 2022.
- [31] Z. Wu, Y. Zhu, and X. Ji, "NiCo₂O₄-based materials for electrochemical supercapacitors," *J Mater Chem A Mater*, vol. 2, no. 36, pp. 14759–14772, 2014.
- [32] D. P. Dubal, P. Gomez-Romero, B. R. Sankapal, and R. Holze, "Nickel cobaltite as an emerging material for supercapacitors: an overview," *Nano Energy*, vol. 11, pp. 377–399, 2015.
- [33] X. Chen, J. Ding, X. Chen, X. Liu, G. Zhuang, and Z. Zhang, "Porous tremella-like NiCo₂S₄ networks electrodes for high-performance dye-sensitized solar cells and supercapacitors," *Solar Energy*, vol. 176, pp. 762–770, 2018.
- [34] X. Cao *et al.*, "Phase exploration and identification of multinary transition-metal selenides as high-efficiency oxygen evolution electrocatalysts through combinatorial electrodeposition," *ACS Catal*, vol. 8, no. 9, pp. 8273–8289, 2018.

- [35] D. Wang *et al.*, “Nickel-cobalt layered double hydroxide nanosheets with reduced graphene oxide grown on carbon cloth for symmetric supercapacitor,” *Appl Surf Sci*, vol. 483, pp. 593–600, 2019.
- [36] A. Voznyi *et al.*, “Structural and electrical properties of SnS₂ thin films,” *Mater Chem Phys*, vol. 173, pp. 52–61, 2016.
- [37] Y. Javed, M. A. Rafiq, and N. Ahmed, “Pressure-induced changes in the electronic structure and enhancement of the thermoelectric performance of SnS₂: a first principles study,” *RSC Adv*, vol. 7, no. 62, pp. 38834–38843, 2017.
- [38] N. Parveen, S. A. Ansari, H. R. Alamri, M. O. Ansari, Z. Khan, and M. H. Cho, “Facile synthesis of SnS₂ nanostructures with different morphologies for high-performance supercapacitor applications,” *ACS Omega*, vol. 3, no. 2, pp. 1581–1588, 2018.
- [39] N. Parveen, S. A. Ansari, H. R. Alamri, M. O. Ansari, Z. Khan, and M. H. Cho, “Facile synthesis of SnS₂ nanostructures with different morphologies for high-performance supercapacitor applications,” *ACS Omega*, vol. 3, no. 2, pp. 1581–1588, 2018.
- [40] D. P. Dubal, O. Ayyad, V. Ruiz, and P. Gomez-Romero, “Hybrid energy storage: the merging of battery and supercapacitor chemistries,” *Chem Soc Rev*, vol. 44, no. 7, pp. 1777–1790, 2015.
- [41] G. Li *et al.*, “Construction of hierarchical NiCo₂O₄@ Ni-MOF hybrid arrays on carbon cloth as superior battery-type electrodes for flexible solid-state hybrid supercapacitors,” *ACS Appl Mater Interfaces*, vol. 11, no. 41, pp. 37675–37684, 2019.
- [42] J. Mayer, P. V Borges, and S. J. Simske, *Fundamentals and applications of hardcopy communication*. Springer, 2018.
- [43] H. Choi and H. Yoon, “Nanostructured electrode materials for electrochemical capacitor applications,” *Nanomaterials*, vol. 5, no. 2, pp. 906–936, 2015.
- [44] P. Simon and Y. Gogotsi, “Materials for electrochemical capacitors,” *Nat Mater*, vol. 7, no. 11, pp. 845–854, 2008.

- [45] S. Mohapatra, A. Acharya, and G. S. Roy, "The role of nanomaterial for the design of supercapacitor," *Lat. Am. J. Phys. Educ*, vol. 6, no. 3, pp. 380–384, 2012.
- [46] A. Burke, Z. Liu, and H. Zhao, "Present and future applications of supercapacitors in electric and hybrid vehicles," in *2014 IEEE International Electric Vehicle Conference (IEVC)*, IEEE, 2014, pp. 1–8.
- [47] M. S. Halper and J. C. Ellenbogen, "Supercapacitors: A brief overview," *The MITRE Corporation, McLean, Virginia, USA*, vol. 1, 2006.
- [48] H. Yang, S. Kannappan, A. S. Pandian, J.-H. Jang, Y. S. Lee, and W. Lu, "Nanoporous graphene materials by low-temperature vacuum-assisted thermal process for electrochemical energy storage," *J Power Sources*, vol. 284, pp. 146–153, 2015.
- [49] A. P. Singh, N. K. Tiwari, P. B. Karandikar, and A. Dubey, "Effect of electrode shape on the parameters of supercapacitor," in *2015 International Conference on Industrial Instrumentation and Control (ICIC)*, IEEE, 2015, pp. 669–673.
- [50] A. G. Pandolfo and A. F. Hollenkamp, "Carbon properties and their role in supercapacitors," *J Power Sources*, vol. 157, no. 1, pp. 11–27, 2006.
- [51] J. M. Boyea, R. E. Camacho, S. P. Sturano, and W. J. Ready, "Carbon nanotube-based supercapacitors: technologies and markets," *Nanotech. L. & Bus.*, vol. 4, p. 19, 2007.
- [52] P. Tamilarasan, A. K. Mishra, and S. Ramaprabhu, "Graphene/ionic liquid binary electrode material for high performance supercapacitor," in *2011 International Conference on Nanoscience, Technology and Societal Implications*, IEEE, 2011, pp. 1–5.
- [53] E. G. Bakhoun and M. H. M. Cheng, "Capacitive pressure sensor with very large dynamic range," *IEEE transactions on components and packaging technologies*, vol. 33, no. 1, pp. 79–83, 2009.
- [54] T. Kim, G. Jung, S. Yoo, K. S. Suh, and R. S. Ruoff, "Activated graphene-based carbons as supercapacitor electrodes with macro-and mesopores," *ACS Nano*, vol. 7, no. 8, pp. 6899–6905, 2013.

- [55] Z. S. Iro, C. Subramani, and S. S. Dash, "A brief review on electrode materials for supercapacitor," *Int. J. Electrochem. Sci*, vol. 11, no. 12, pp. 10628–10643, 2016.
- [56] E. Frackowiak, V. Khomenko, K. Jurewicz, K. Lota, and F. Béguin, "Supercapacitors based on conducting polymers/nanotubes composites," *J Power Sources*, vol. 153, no. 2, pp. 413–418, 2006.
- [57] F. Shi, L. Li, X. Wang, C. Gu, and J. Tu, "Metal oxide/hydroxide-based materials for supercapacitors," *RSC Adv*, vol. 4, no. 79, pp. 41910–41921, 2014.
- [58] V. Augustyn, P. Simon, and B. Dunn, "Pseudocapacitive oxide materials for high-rate electrochemical energy storage," *Energy Environ Sci*, vol. 7, no. 5, pp. 1597–1614, 2014.
- [59] S. Vijayakumar, S. Nagamuthu, and G. Muralidharan, "Supercapacitor studies on NiO nanoflakes synthesized through a microwave route," *ACS Appl Mater Interfaces*, vol. 5, no. 6, pp. 2188–2196, 2013.
- [60] C. Yuan, L. Yang, L. Hou, L. Shen, X. Zhang, and X. W. D. Lou, "Growth of ultrathin mesoporous Co₃O₄ nanosheet arrays on Ni foam for high-performance electrochemical capacitors," *Energy Environ Sci*, vol. 5, no. 7, pp. 7883–7887, 2012.
- [61] C.-C. Hu, J.-C. Chen, and K.-H. Chang, "Cathodic deposition of Ni(OH)₂ and Co(OH)₂ for asymmetric supercapacitors: importance of the electrochemical reversibility of redox couples," *J Power Sources*, vol. 221, pp. 128–133, 2013.
- [62] N. Choudhary *et al.*, "Asymmetric supercapacitor electrodes and devices," *Advanced Materials*, vol. 29, no. 21, p. 1605336, 2017.
- [63] Z. Lu, Z. Chang, W. Zhu, and X. Sun, "Beta-phased Ni(OH)₂ nanowall film with reversible capacitance higher than theoretical Faradic capacitance," *Chemical Communications*, vol. 47, no. 34, pp. 9651–9653, 2011.

- [64] M. Setayeshmehr, M. Haghghi, and K. Mirabbaszadeh, "A review of tin disulfide (SnS₂) composite electrode materials for supercapacitors," *Energy Storage*, vol. 4, no. 4, p. e295, 2022.
- [65] Y. Wang, P. He, W. Lei, F. Dong, and T. Zhang, "Novel FeMoO₄/graphene composites based electrode materials for supercapacitors," *Compos Sci Technol*, vol. 103, pp. 16–21, 2014.
- [66] Y. Zhang, L. Li, H. Su, W. Huang, and X. Dong, "Binary metal oxide: advanced energy storage materials in supercapacitors," *J Mater Chem A Mater*, vol. 3, no. 1, pp. 43–59, 2015.
- [67] Q. Wang *et al.*, "Morphology evolution of urchin-like NiCo₂O₄ nanostructures and their applications as pseudocapacitors and photoelectrochemical cells," *J Mater Chem*, vol. 22, no. 40, pp. 21647–21653, 2012.
- [68] D. Guo, Y. Luo, X. Yu, Q. Li, and T. Wang, "High performance NiMoO₄ nanowires supported on carbon cloth as advanced electrodes for symmetric supercapacitors," *Nano Energy*, vol. 8, pp. 174–182, 2014.
- [69] H. Liang, Z. Wei, J. Xiang, H. Xu, G. Li, and Y. Huang, "Hierarchical core-shell NiCo₂O₄@ NiMoO₄ nanowires grown on carbon cloth as integrated electrode for high-performance supercapacitors. Sci. Rep. 6, 31465 (2016)." 2016.
- [70] Y. C. Zhang, J. Li, M. Zhang, and D. D. Dionysiou, "Size-tunable hydrothermal synthesis of SnS₂ nanocrystals with high performance in visible light-driven photocatalytic reduction of aqueous Cr (VI)," *Environ Sci Technol*, vol. 45, no. 21, pp. 9324–9331, 2011.
- [71] S. S. Rabbani *et al.*, "Mesoporous NiCo₂S₄ nanoflakes as an efficient and durable electrocatalyst for non-enzymatic detection of cholesterol," *Nanotechnology*, vol. 33, no. 37, p. 375502, 2022.
- [72] N. Parveen, S. A. Ansari, H. R. Alamri, M. O. Ansari, Z. Khan, and M. H. Cho, "Facile synthesis of SnS₂ nanostructures with different morphologies for high-performance supercapacitor applications," *ACS Omega*, vol. 3, no. 2, pp. 1581–1588, 2018.

- [73] H. Chen *et al.*, “In-situ grown SnS₂ nanosheets on rGO as an advanced anode material for lithium and sodium ion batteries,” *Front Chem*, vol. 6, p. 629, 2018.
- [74] H. Wu, M. Qin, and L. Zhang, “NiCo₂O₄ constructed by different dimensions of building blocks with superior electromagnetic wave absorption performance,” *Compos B Eng*, vol. 182, p. 107620, 2020.
- [75] A. Manalu *et al.*, “Synthesis, Microstructure and Electrical Properties of NiCo₂O₄/rGO Composites as Pseudocapacitive Electrode for Supercapacitors,” *Int J Electrochem Sci*, vol. 17, no. 3, p. 22036, 2022.
- [76] U. T. Nakate and S. N. Kale, “Microwave assisted synthesis and characterizations of NiCo₂O₄ nanoplates and electrical, magnetic properties,” *Mater Today Proc*, vol. 3, no. 6, pp. 1992–1998, 2016.
- [77] S. Zheng, Y.-L. Song, S.-X. Wang, L.-Z. Wang, and J. Yan, “Synthesis of dragon fruit tree-like hierarchical NiCo₂O₄ growth on carbon cloth and its supercapacitive performance,” *Results Phys*, vol. 14, p. 102441, 2019.
- [78] Z. Ren *et al.*, “Rational design of layered SnS₂ on ultralight graphene fiber fabrics as binder-free anodes for enhanced practical capacity of sodium-ion batteries,” *Nanomicro Lett*, vol. 11, pp. 1–12, 2019.
- [79] M. Hussain *et al.*, “Ni and Co synergy in bimetallic nanowires for the electrochemical detection of hydrogen peroxide,” *Nanotechnology*, vol. 32, no. 20, p. 205501, 2021.
- [80] Y. Li *et al.*, “Unveiling the dynamic capacitive storage mechanism of Co₃O₄@NiCo₂O₄ hybrid nanoelectrodes for supercapacitor applications,” *Electrochim Acta*, vol. 145, pp. 177–184, 2014.
- [81] H. Chen *et al.*, “In-situ grown SnS₂ nanosheets on rGO as an advanced anode material for lithium and sodium ion batteries,” *Front Chem*, vol. 6, p. 629, 2018.

- [82] X. Cai, W. Sun, C. Xu, L. Cao, and J. Yang, “Highly selective catalytic reduction of NO via SO₂/H₂O-tolerant spinel catalysts at low temperature,” *Environmental Science and Pollution Research*, vol. 23, pp. 18609–18620, 2016.
- [83] M. Sethi and D. K. Bhat, “Facile solvothermal synthesis and high supercapacitor performance of NiCo₂O₄ nanorods,” *J Alloys Compd*, vol. 781, pp. 1013–1020, 2019.
- [84] B. Saravanakumar, T. Priyadharshini, G. Ravi, V. Ganesh, A. Sakunthala, and R. Yuvakkumar, “Hydrothermal synthesis of spherical NiCO₂O₄ nanoparticles as a positive electrode for pseudocapacitor applications,” *J Solgel Sci Technol*, vol. 84, pp. 297–305, 2017.
- [85] X. Liu, J. Zeng, H. Yang, K. Zhou, and D. Pan, “V₂O₅-Based nanomaterials: synthesis and their applications,” *RSC Adv*, vol. 8, no. 8, pp. 4014–4031, 2018.
- [86] H. Xia, J. Zhang, Z. Yang, S. Guo, S. Guo, and Q. Xu, “2D MOF nanoflake-assembled spherical microstructures for enhanced supercapacitor and electrocatalysis performances,” *Nanomicro Lett*, vol. 9, pp. 1–11, 2017.
- [87] H. Chauhan, M. K. Singh, P. Kumar, S. A. Hashmi, and S. Deka, “Development of SnS₂/RGO nanosheet composite for cost-effective aqueous hybrid supercapacitors,” *Nanotechnology*, vol. 28, no. 2, p. 025401, 2016.
- [88] R. K. Mishra, G. W. Baek, K. Kim, H.-I. Kwon, and S. H. Jin, “One-step solvothermal synthesis of carnation flower-like SnS₂ as superior electrodes for supercapacitor applications,” *Appl Surf Sci*, vol. 425, pp. 923–931, 2017.
- [89] L. Ma, L. Xu, X. Zhou, X. Xu, and L. Zhang, “Molybdenum-doped few-layered SnS₂ architectures with enhanced electrochemical supercapacitive performance,” *RSC Adv*, vol. 5, no. 128, pp. 105862–105868, 2015.
- [90] S. Anand *et al.*, “Flexible nickel disulfide nanoparticles-anchored carbon nanofiber hybrid mat as a flexible binder-free cathode for solid-state asymmetric supercapacitors,” *Nanotechnology*, vol. 32, no. 49, p. 495403, 2021.

- [91] X. Zhang *et al.*, “NiFe₂O₄ nanocubes anchored on reduced graphene oxide cryogel to achieve a 1.8 V flexible solid-state symmetric supercapacitor,” *Chemical Engineering Journal*, vol. 360, pp. 171–179, 2019.
- [92] S. Asaithambi *et al.*, “Synthesis and characterization of various transition metals doped SnO₂@ MoS₂ composites for supercapacitor and photocatalytic applications,” *J Alloys Compd*, vol. 853, p. 157060, 2021.
- [93] Z. Wang *et al.*, “Electrospinning CoS₂/carbon nanofibers with enhanced stability as electrode materials for supercapacitors,” *Ionics (Kiel)*, vol. 26, pp. 5737–5746, 2020.
- [94] X. Chen, J. Ding, X. Chen, X. Liu, G. Zhuang, and Z. Zhang, “Porous tremella-like NiCo₂S₄ networks electrodes for high-performance dye-sensitized solar cells and supercapacitors,” *Solar Energy*, vol. 176, pp. 762–770, 2018.
- [95] X. He *et al.*, “Flexible binder-free hierarchical copper sulfide/carbon cloth hybrid supercapacitor electrodes and the application as negative electrodes in asymmetric supercapacitor,” *Journal of Materials Science: Materials in Electronics*, vol. 31, pp. 2145–2152, 2020.
- [96] D. Wang *et al.*, “Nickel-cobalt layered double hydroxide nanosheets with reduced graphene oxide grown on carbon cloth for symmetric supercapacitor,” *Appl Surf Sci*, vol. 483, pp. 593–600, 2019.